AFRL-VA-WP-TR-2001-3020

ENHANCEMENTS TO REPAIR ASSESSMENT PROCEDURE AND INTEGRATED DESIGN (RAPID) FOR ANTENNA CUTOUTS

Delivery Order 0007: Analysis Methods Enhancements

Chun C. Chen
Miles Nomura
Jin Yu

The Boeing Company
2401 E. Wardlow Road
Long Beach, CA 90807-5309

JUNE 2001

FINAL REPORT FOR 01 MARCH 1999 – 31 MARCH 2000

AIR VEHICLES DIRECTORATE
AIR FORCE RESEARCH LABORATORY
AIR FORCE MATERIEL COMMAND
WRIGHT-PATTERSON AIR FORCE BASE, OH 45433-7542

NOTICE

USING GOVERNMENT DRAWINGS, SPECIFICATIONS, OR OTHER DATA INCLUDED IN THIS DOCUMENT FOR ANY PURPOSE OTHER THAN GOVERNMENT PROCUREMENT DOES NOT IN ANY WAY OBLIGATE THE US GOVERNMENT. THE FACT THAT THE GOVERNMENT FORMULATED OR SUPPLIED THE DRAWINGS, SPECIFICATIONS, OR OTHER DATA DOES NOT LICENSE THE HOLDER OR ANY OTHER PERSON OR CORPORATION; OR CONVEY ANY RIGHTS OR PERMISSION TO MANUFACTURE, USE, OR SELL ANY PATENTED INVENTION THAT MAY RELATE TO THEM.

THIS REPORT IS RELEASABLE TO THE NATIONAL TECHNICAL INFORMATION SERVICE (NTIS). AT NTIS, IT WILL BE AVAILABLE TO THE GENERAL PUBLIC, INCLUDING FOREIGN NATIONS.

THIS TECHNICAL REPORT HAS BEEN REVIEWED AND IS APPROVED FOR PUBLICATION.

Michael T. Myers

MICHAEL T. MYERS, Capt, UASF
Lead Engineer, Aircraft Repair
Analytical Structural Mechanics Branch

David M Agins

DAVID M. AGINS, Maj, USAF
Chief, Analytical Structural Mechanics Branch
Structures Division

JEFFREY S. TURCOTTE, LTC, USAF
Deputy Chief
Structures Division

Do not return copies of this report unless contractual obligations or notice on a specific document requires its return.

REPORT DOCUMENTATION PAGE

Form Approved
OMB No. 0704-0188

1. REPORT DATE *(DD-MM-YY)*	2. REPORT TYPE	3. DATES COVERED *(From - To)*
June 2001	Final	03/01/1999 – 03/31/2000

4. TITLE AND SUBTITLE

ENHANCEMENTS TO REPAIR ASSESSMENT PROCEDURE AND INTEGRATED DESIGN (RAPID) FOR ANTENNA CUTOUTS

Delivery Order 0007: Analysis Methods Enhancements

5a. CONTRACT NUMBER F33615-95-D-3217

5b. GRANT NUMBER

5c. PROGRAM ELEMENT NUMBER 69199F

6. AUTHOR(S)

Chun C. Chen
Miles Nomura
Jin Yu

5d. PROJECT NUMBER GOVF

5e. TASK NUMBER 02

5f. WORK UNIT NUMBER 02

7. PERFORMING ORGANIZATION NAME(S) AND ADDRESS(ES)

The Boeing Company
2401 E. Wardlow Road
Long Beach, CA 90807-5309

8. PERFORMING ORGANIZATION REPORT NUMBER

CRAD-9909-TR-6428

9. SPONSORING/MONITORING AGENCY NAME(S) AND ADDRESS(ES)

AIR VEHICLES DIRECTORATE
AIR FORCE RESEARCH LABORATORY
AIR FORCE MATERIEL COMMAND
WRIGHT-PATTERSON AIR FORCE BASE, OH 45433-7542

10. SPONSORING/MONITORING AGENCY ACRONYM(S) AFRL/VASM

11. SPONSORING/MONITORING AGENCY REPORT NUMBER(S) AFRL-VA-WP-TR-2001-3020

12. DISTRIBUTION/AVAILABILITY STATEMENT

Approved for public release; distribution is unlimited.

13. SUPPLEMENTARY NOTES

14. ABSTRACT *(Maximum 200 Words)*

This report describes static strength and damage tolerance analysis methods for skin modifications to antenna installations on the fuselage of commuter airplanes. The methods are implemented in the design and analysis program of RAPID for commuters (RAPIDC). First, three types of antenna installations are presented, defined in terms of the mounting plate geometry. The applicability of antenna systems within the analysis capability of RAPIDC is addressed next. Finally, the static strength and damage tolerance analysis procedures are described. The damage tolerance analysis procedure is demonstrated through an illustrative example.

15. SUBJECT TERMS

Aircraft repair, Bolted repairs, Antenna installation, Computer repair design tool, Design and analysis, Damage tolerance, Commuter aircraft repair

16. SECURITY CLASSIFICATION OF:			17. LIMITATION OF ABSTRACT:	18. NUMBER OF PAGES	19a. NAME OF RESPONSIBLE PERSON (Monitor)
a. REPORT	b. ABSTRACT	c. THIS PAGE			Edward Schopler
Unclassified	Unclassified	Unclassified	SAR	68	19b. TELEPHONE NUMBER *(Include Area Code)* (937) 656-5755

Table of Contents

Summary

Static strength and damage tolerance analysis methods for skin modifications to antenna installations on the fuselage of commuter airplanes are described in this report. The methods are implemented in the analysis program of RAPIDC Version 1.0 for commuters. Three types of antenna installation in terms of the shapes of mounting plate are first defined. The applicability of antenna systems within the analysis capability of RAPIDC is next addressed. Static strength and damage tolerance analysis procedures are then described. The damage tolerance analysis procedure is demonstrated through an illustrative example.

1.0 RAPIDC Capabilities

The analysis of a modified fuselage skin to antenna installation in RAPIDC for commuter airplanes is an addition to the RAPID program originally developed for common repairs to large transport aircraft. The analysis capability of RAPIDC Version 1.0 for antenna installations is limited to the types and systems described below.

1.1 Types of Antenna Installation

Three common types of antenna installation are considered. They differ only in the shapes of mounting plates: rectangular, circular, and elliptical shape as shown in Figure 1. The mounting plates are mechanically fastened to the skin around the cutout.

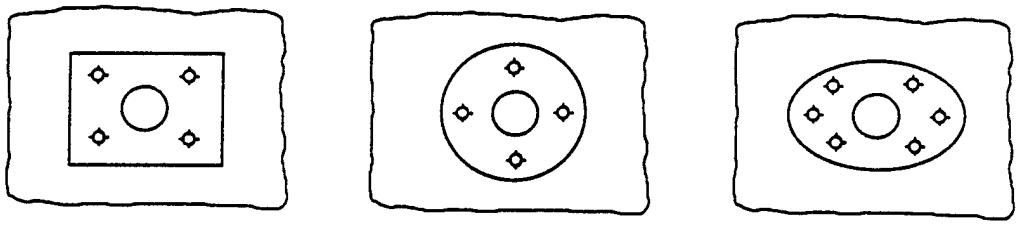

(a) Rectangular (b) Circular (c) Elliptical

Figure 1. Three types of antenna installation

In RAPIDC Version 1.0, only the circular and rectangular installations are considered. The elliptical installations will be included in the next version release.

1.2 Antenna System Applicability

RAPIDC Version 1.0 excludes the case of skin bending that is induced by antenna vibrations subjected to aerodynamic loading. Therefore, communication antennas (typically 5" long by 3" wide by 10" tall) are excluded. However, antenna systems such as ADF (12" long by 6" wide by 1" tall), GPS (4" long by 4"

wide by 0.5" tall), Transponder and DME (5" long by 2" wide by 4" tall), and TCAS are covered in the analysis.

2.0 Static Strength Analysis

Typical antenna installations on the fuselage of commuter airplanes generally involve cutting a hole in the skin for the antenna connector. A mounting plate is then mechanically fastened to the skin around the skin cutout. To assess the static strength of the modified skin, three independent criteria are used to evaluate the margins of safety of the mounting plate and fasteners: the mounting plate allowable, the joint allowable, and the shear allowable.

2.1 The Mounting Plate Allowable and Margin of Safety

To assess the loss of skin strength due to antenna connector hole cutout, the margin of safety of the mounting plate is calculated as

$$\text{Margin of Safety} = \frac{P_{pu}}{P_p} - 1$$

where P_{pu}, the mounting plate load allowable, is calculated using the equation

$$P_{pu} = F_{tu} (w_p - D)\, t_p$$

in which F_{tu}, w_p, D, and t_p are the ultimate tensile strength, width, cutout diameter, and thickness of the mounting plate, respectively.

The skin internal force, P_p , is calculated using the equation

$$P_p = \sigma_u D\, t_s$$

where σ_u and t_s are the design ultimate tensile stress and thickness of the skin, respectively.

2.2 The Fastener Joint Allowable and Margin of Safety

In the vicinity of an antenna installation on the skin, skin stresses are transferred to the mounting plate through fasteners via fastener shear and hole bearing. The fastener together with the skin and mounting plate represents a fastener joint. A joint can only transfer a certain amount of load until it fails. The point at which this fastener joint fails is the joint allowable. The calculation of the joint allowable is based upon two loading conditions, fastener shear and hole bearing. Two hole types also have to be considered when determining the joint allowable, the straight shank and countersunk.

2.2.1 Fastener Joint Allowable in Straight Shank Holes

Straight shank holes are used for protruding head fasteners and for the mounting plate that have a flush head fastener installed but are not countersunk. The joint allowable is the lower of the shear allowable or the hole bearing allowable. An allowable is calculated for the skin and mounting plate that the fastener goes through.

The single shear allowable for straight shank holes is calculated using the following equation

$$P_{su} = F_{su} \times A_f \times S_{CF1}$$

The mounting plate shear allowable for straight shank holes is calculated using the following equation

$$P_{su} = 2 \times F_{su} \times A_f \times S_{CF2}$$

In both equations, F_{su} is the ultimate shear strength of the fastener material, A_f is the cross-sectional area of each fastener, S_{CF1} is the single shear correction factor and S_{CF2} is the double shear correction factor. S_{CF1} and S_{CF2} are used only for solid rivets and can be found in MIL-Handbook 5F Table 8.1.2.1(b).

The hole bearing allowable for the straight shank hole is calculated using the following equation

$$P_{bru} = F_{bru} \times d \times t$$

in which F_{bru} is the ultimate bearing stress of the plate (skin or mounting plate) material, d is the fastener hole diameter, and t is the thickness. Currently, the F_{bru} is for the case E/D (edge distance to hole diameter) equal to 2.0.

The joint allowable for a given joint is the lower of P_{su} or P_{bru}denoted by P_{joint}.

2.2.2 Fastener Joint Allowable in Countersunk Holes

The fastener joint allowables for countersunk holes are different from the straight shank holes. They are determined by tests and can be found in MIL-Handbook 5F Section 8.

2.2.3 Fastener Joint Margin of Safety

The fastener joint margin of safety is determined by summing each fastener joint allowable in the skin and mounting plate, and this is done for each side of the mounting plate.

$$P_{total} = \sum_{n=1}^{K} (P_{joint})_n$$

in which P_{total} is the total fastener joint load, $(P_{joint})_n$ is the fastener joint load for the nth fastener and K is the number of fasteners.

The P_{total} for the skin and mounting are then compared. The smaller of the two is the fastener joint allowable for that side of the mounting plate and is used in determining the margin of safety for the fastener joints.

An applied load is needed to determine a margin of safety. That load is the ultimate applied load to the structure, or if that is not known, then the tensile ultimate strength of the material F_{tu} is used. This applied load $P_{applied}$ is given by

$$P_{applied} = \sigma_u D t_s$$

where σ_u is either the design ultimate tensile stress or the tensile ultimate skin strength, t_s is the skin thickness, D is the diameter of antenna connector cutout hole. The margin of safety is given by

$$\text{Margin of Safety} = \frac{P_{total}}{P_{applied}} - 1$$

2.3 The Shear Margin of Safety

The shear margin of safety of the antenna installation is calculated by

$$\text{Margin of Safety} = \frac{(F_{SU}\, t)_p}{(F_{SU}\, t)_s} - 1$$

where F_{SU} is the ultimate shear strength of the skin or mounting plate material. The equation is used for each side of the mounting plate.

2.4 Margin of Safety as a Criterion

The margins of safety (MS) based on the mounting plate allowable and the fastener joint allowable were calculated to determine the adequacy of the antenna installation on fuselage skin.

- MS < 0 Antenna installation is statically inadequate
- MS = 0 Antenna installation is marginally adequate
- MS > 0 Antenna installation is statically adequate

For antenna installations that are not statically adequate, they must be redesigned to ensure the adequacy of the antenna installation.

2.5 The Stiffness Check of the Antenna Installation

The stiffness ratio between the mounting plate and the skin is calculated using the following equation

$$\text{Stiffness Ratio} = \frac{(E\,t)_p}{(E\,t)_s}$$

The antenna installation is considered adequate if the ratio is between 1.0 and 1.5. The antenna installation is too stiff when the value is greater than 1.5 and not stiff enough when it is less than 1.0.

2.6 The Fastener Bending Check of the Antenna Installation

The fastener bending is checked using the following equation

$$Q = \frac{t_s + t_p}{d}$$

Where d is the fastener diameter, t_s and t_p are the thickness of skin and mounting plate, respectively. The parameter Q is the fastener bending indicator. For aluminum fasteners, the bending is important. A Q value above 2 may indicate that the aluminum rivet will not fill the hole but instead may buckle in the hole. In such a case, RAPIDC recommends steel or titanium fasteners be used. For steel and titanium fasteners, there is no constraint for typical fuselage antenna installations.

2.7 The Inter-Rivet Buckling Guideline

To avoid inter-rivet buckling in the modified skin, the fastener spacing should be four to six times the diameter of the fastener shank diameter. This guideline is enforced during user input phase of RAPIDC.

3.0 Damage Tolerance Analysis

To perform the damage tolerance analysis of a modified skin for antenna installations, critical locations in the skin must first be determined. Assumptions of initial flaws at fracture critical locations and the continuing damage need to be made. The stress spectrum must also be prescribed. In addition, the following data are needed:

- Crack growth rate data of the skin material
- Fracture toughness of the skin material
- Stress intensity factors of relevant crack configurations

Damage tolerance analysis procedure is described in the flowchart shown in Figure 2. Each element in the analysis procedure is described as follows.

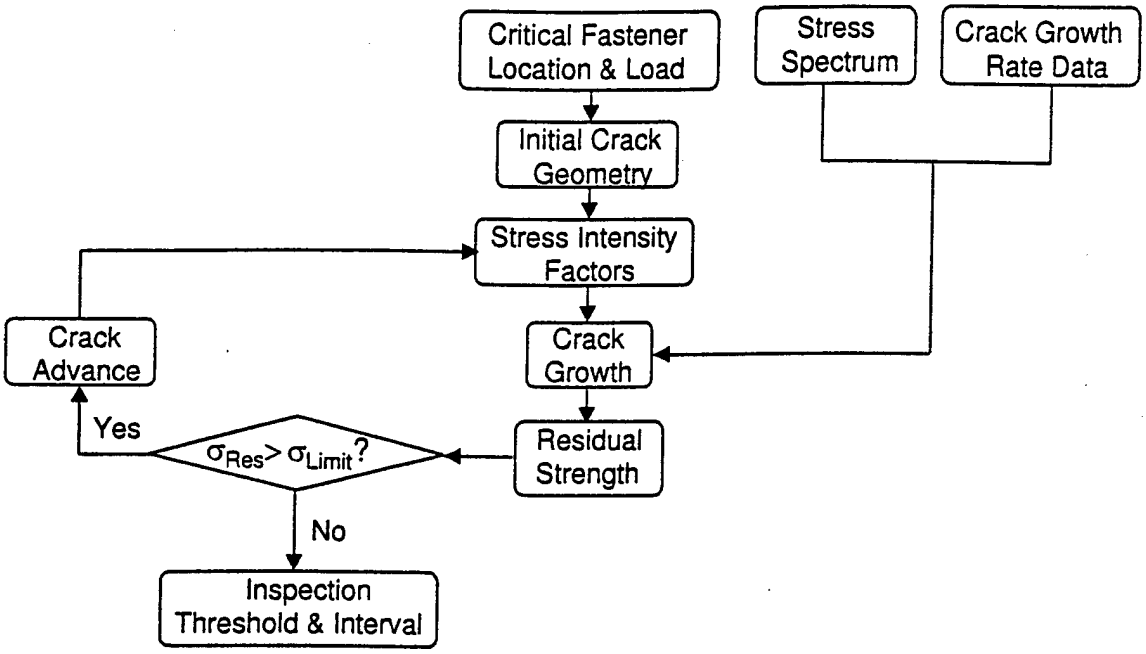

Figure 2. Flow Chart of Damage Tolerance Analysis Procedure

3.1 Critical Fastener Locations

Damage tolerance analysis of the modified skin begins by postulating the initial flaws at the critical locations. For rectangular installations, two locations are identified at the center and corner fastener holes in the outermost fastener rows that have higher load transfer. A third location is identified at the edge of antenna connector hole cutout in the skin where stress concentration is the highest. For circular installations, the critical locations are identified at the top or bottom fastener in the outermost ring and at the antenna connector hole cutout as well. The critical fastener locations in circular and rectangular installations are indicated in Figure 3.

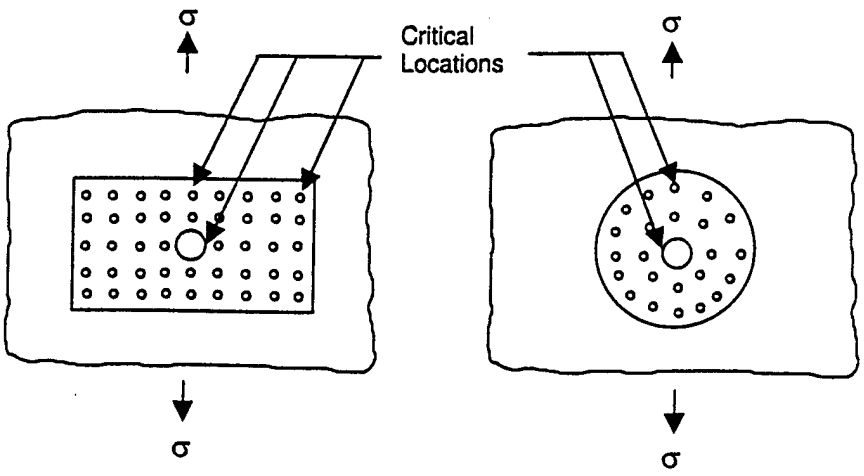

Figure 3. Critical Fastener Locations

3.2 Fastener Loads and Skin Stress Gradients

The fastener loads or skin stress gradients along the potential crack growth path are needed for calculating crack tip stress intensity factors. The determination of fastener loads and skin stress gradients was accomplished using the FRANC2D/L program developed jointly at Cornell University and Kansas State University sponsored by NASA-Langley Research center. The finite element model was created using the FRANC2D/L preprocessor program called CASCA developed at Cornell University.

In FRANC2D/L analysis, the fastener shear rigidity needs to be calculated separately and input into the program. The FRANC2D/L program then assembles stiffnesses contributing from skin, mounting plate, and fasteners to form the overall stiffness matrix. The shear rigidity can be calculated using the Swift's empirical equation:

$$K = \frac{E\,d}{A + B\left(\frac{d}{t_{Skin}} + \frac{d}{t_{MountingPlate}}\right)}$$

where E is the weighted Young's modules of the skin and mounting plate, d is the fastener hole diameter, t_{Skin} and $t_{Mounting\ Plate}$ are the thickness of the skin and mounting plate, respectively, and A and B are material dependent empirical constants. The values of A and B, for aluminum fasteners, are 5.0 and 0.8, respectively.

In RAPIDC, databases of fastener loads and skin stress gradients along the potential crack growth path are developed for circular and rectangular installations. Parameters considered include:

Skin thickness: 0.032", 0.040", 0.050", and 0.063"
Mounting plate thickness: 1 gauge higher than skin thickness
Cutout diameter: 1.0", 2.0", and 3.0"
Fastener size: 1/8", 5/32", and 3/16"
Number of fastener rows: 1 ~ 5
Aspect ratio: 1:1 (square), 1:1.3 and 1:1.6
Materials: Aluminum skin and mounting plate
Aluminum fastener

Fastener loads and skin stress gradients calculations along the potential crack growth paths are described in Appendix A.

3.3 Initial Flaw Size and Subsequent Growth Scenarios

To simplify the damage tolerance analysis of the modified skin, initial flaws and their growth pattern were assumed. Three scenarios are considered in RAPIDC for rectangular antenna installations, according to the decision made in a technical review meeting (September 22, 1999 in Albuquerque, New Mexico), and are described below in Figure 4.

Scenario 1: Center fastener hole in the outermost fastener row

Initial Crack: Two diametric through cracks of lengths 0.05" and 0.005", respectively, emanating from the center fastener hole together with a 0.005" crack at one side of every other hole

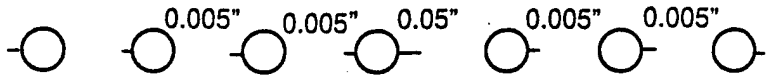

Subsequent Damage: All cracks grow concurrently but independently, interaction between cracks being ignored. The amount of growth δa_1 for the 0.005" crack is added to its original length when the 0.05" crack grows into the adjacent hole. The same process continues in successive growth.

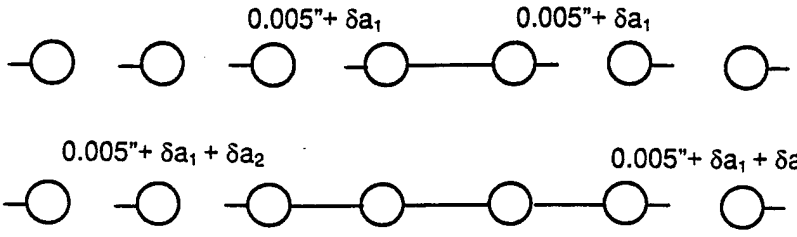

Scenario 2: Corner fastener hole in the outermost fastener row

Initial Crack: Two diametric through cracks of lengths 0.05", pointing toward the adjacent hole, and 0.005", respectively, emanating from the corner fastener hole together with a 0.005" crack at one side of every other hole

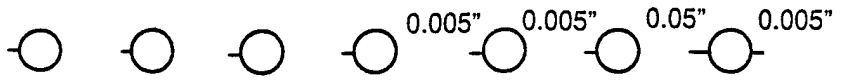

Subsequent Damage: All cracks grow concurrently but independently, without interaction between cracks being considered. The amount of growth δa for the 0.005" crack is added to its original length when the 0.05" crack grows into the adjacent hole. The same process continues in successive growth.

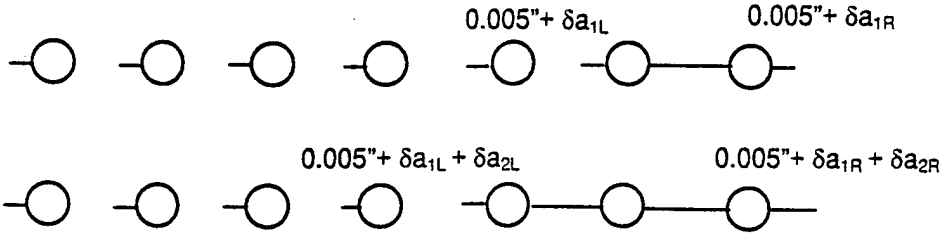

It is noted that successive growths of the 0.005" at corner fastener hole δa_{1R}, δa_{2R}, etc. are different from the growths at other holes δa_{1L}, δa_{2L}, etc. because the former does not grow toward an adjacent hole but others do.

Scenario 3: Antenna connector hole

Initial Crack: Two diametric through cracks of lengths 0.05" and 0.005", respectively, emanating from the antenna connector hole together with a 0.005" crack at one side of every other hole

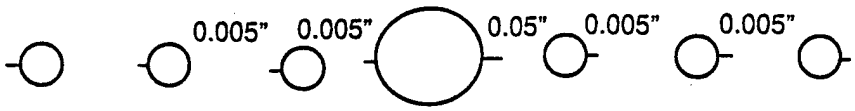

Subsequent Damage: All cracks grow concurrently but independently, ignoring interaction between cracks. The amount of growth δa for the 0.005" crack is added to its original length when the 0.05" crack grows into the adjacent hole. The same process continues in successive growth.

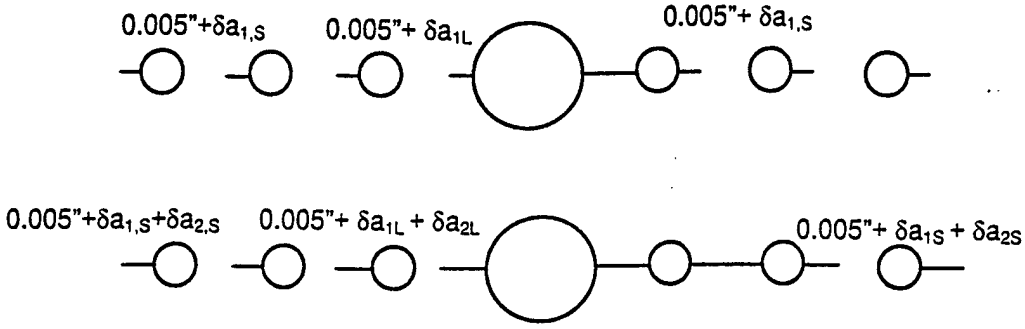

It is noted that successive growths of the 0.005" at antenna connector hole δa_{1L}, δa_{2L}, etc. are different from the growths of 0.005" crack at fastener holes δa_{1S}, δa_{2S}, etc. because the hole sizes and fastener pitches are different.

Figure 4. Initial Flaws and Subsequent Growths Assumptions

For circular antenna installations, two scenarios are considered. The first scenario postulates two initial diametric cracks with 0.05" and 0.005" at the top or bottom fastener in the outermost ring. The cracks grow concurrently but independently in the skin. The second scenario is the same as Scenario 3 for the rectangular antenna installation.

3.4 Stress Intensity Factors

In RAPIDC, stress intensity factors are calculated using three methods. For a crack emanating from a pin-loaded fastener hole in the skin, the stress intensity factor is calculated from the gross, bearing, and bypass stresses using the superposition method. For a crack emanating from the antenna connector open hole in the skin, it is calculated from stress gradients using the weight function method. To account for the hole effect as a crack is growing toward the adjacent hole, an engineering approach which compounds geometry factors is used. These methods are described below.

Method 1: Superposition method

As the method implied, the stress intensity factor for a crack emanating from a hole in a plate subjected to gross, bearing, and bypass stresses can be obtained using the superposition method as illustrated in Figure 5.

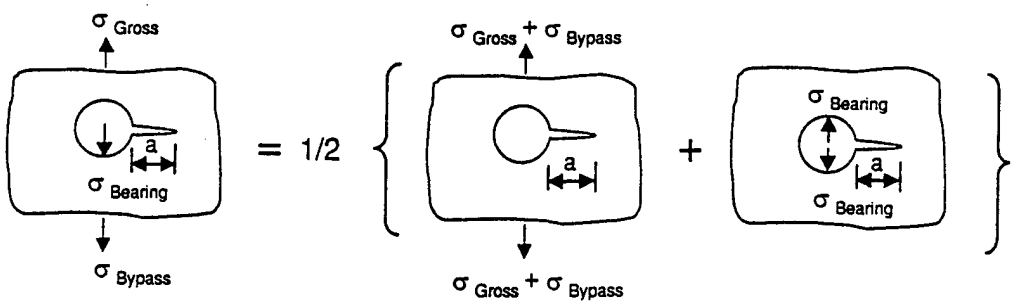

Figure 5. Superposition of Stress Intensity Factors

Let BRF and BPF denote the bearing factor ($\sigma_{Bearing}$ / σ_{Gross}) and the bypass factor, (σ_{Bypass} / σ_{Gross}), respectively. The stress intensity factor K can be calculated by

$$K = K_{Far\ Field} + K_{Point\ Loads}$$

$$= \tfrac{1}{2}(1+BPF)\,\sigma_{Gross}\sqrt{\pi a}\,\beta_{FarField} + \tfrac{1}{2}\,BRF\,\sigma_{Gross}\sqrt{\pi a}\,\beta_{PointLoads}$$

$$= \tfrac{1}{2}\left[(1+BPF)\,\beta_{FarField} + BRF\,\beta_{PointLoads}\right]\sigma_{Gross}\sqrt{\pi a}$$

In the above equation, $\beta_{Far\ Field}$ and $\beta_{Point\ Loads}$ are the geometry factors (or β factors) which are the normalized stress intensity factors of a crack at a hole in a wide plate subjected to a unit far field stress and unit bearing stress divided by $\sqrt{\pi a}$, respectively. The crack length "a" is measured from the crack tip to the edge of the hole.

The stress intensity factor K is divided by K_o to obtain the geometry factor β as

$$\beta = K / K_o$$

$$= \tfrac{1}{2}\left[\,(1 + BPF)\,\beta_{Far\ Field} + BRF\,\beta_{Point\ Loads}\,\right]$$

where K_o is the stress intensity factor of a crack at a hole in a wide plate subjected to a gross stress σ_{Gross}, i.e., $K_o = \sigma_{Gross}\sqrt{\pi a}$.

To calculate the geometry factor β, the geometry factors $\beta_{Far\ Field}$ and $\beta_{Point\ Loads}$ are needed. Shown in Figures 6 and 7 are geometry factors $\beta_{Far\ Field}$ and $\beta_{Point\ Loads}$, respectively.

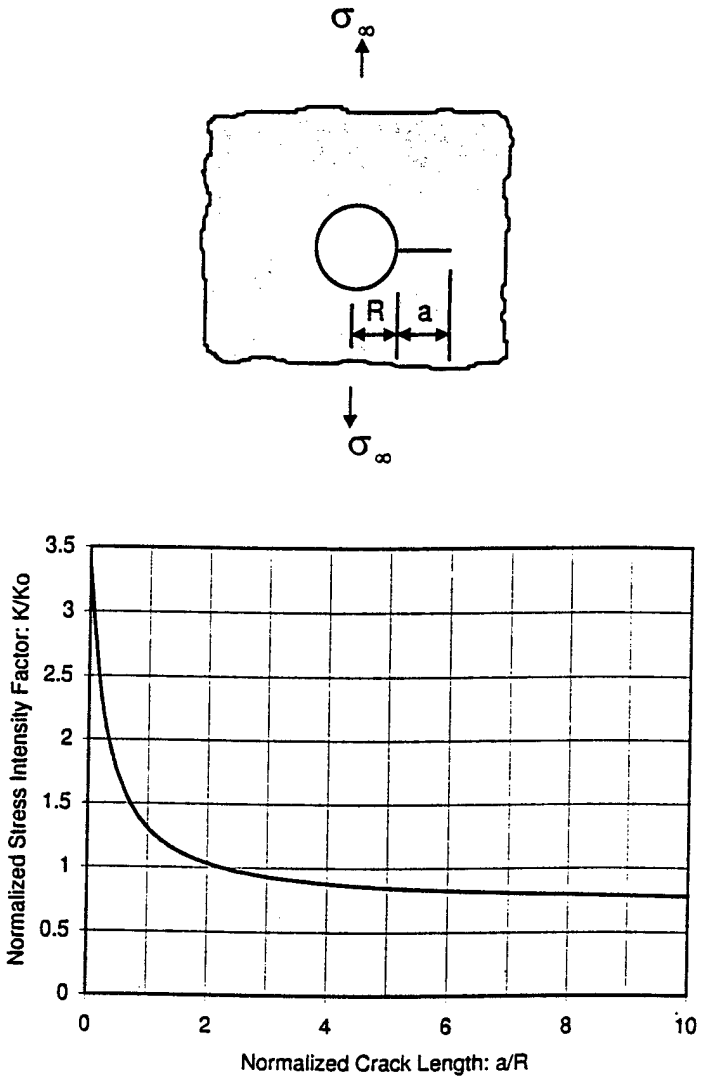

Figure 6. A Crack Emanating from a Hole under Uniform Far Field Stress: $K_o = \sigma_\infty \sqrt{\pi a}$

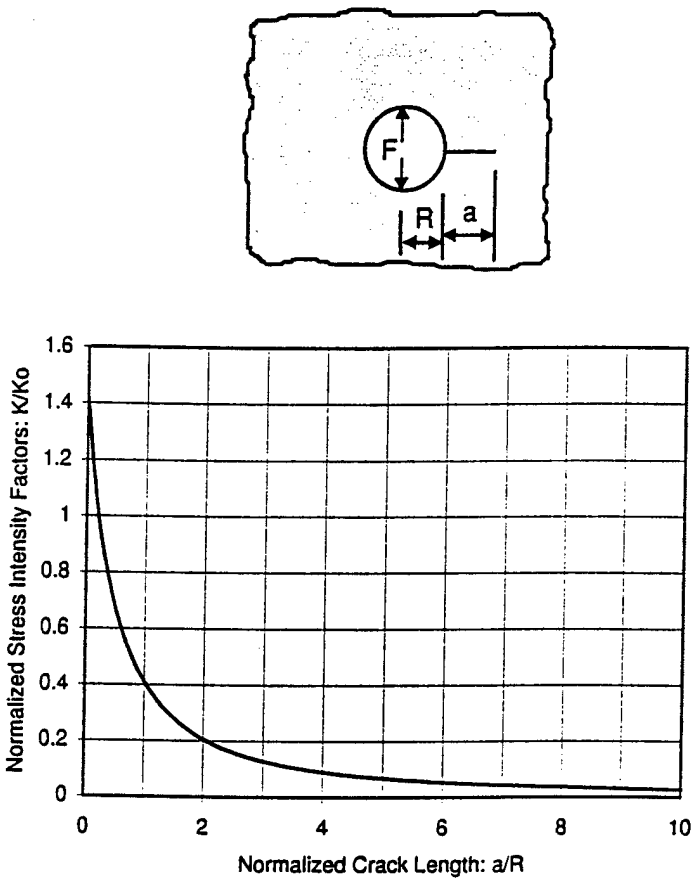

Figure 7. A Crack Emanating from a Hole under a Pair of Point Loads: $K_o = \frac{F}{2Rt}\sqrt{\pi a}$

Method 2: Weight function method

The stress intensity factor of a crack emanating from a hole in a wide plate subjected to stress gradients on crack faces as shown in Figure 8(a) can be calculated using the weight function method. In this case, the stress intensity factor is obtained by summing up stress intensity factors for each pair of point loads acting on crack faces at a distance x from the edge of the hole as shown in Figure 8(b).

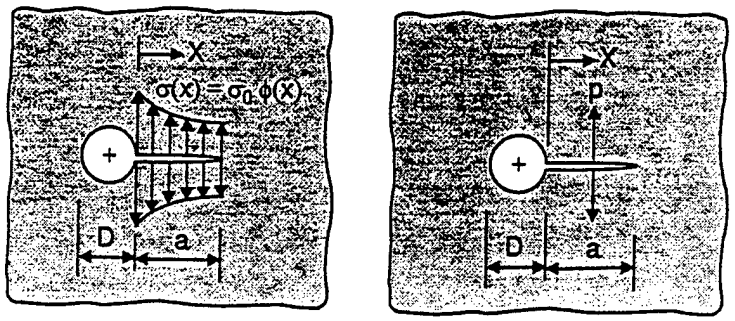

(a) Stress Gradients (b) A Pair of Point Loads

Figure 8. Illustration of the Weight Function Method

Suppose the stress intensity factor of the crack geometry subjected to the load condition described in Figure 8(b) is known as

$$\Delta K(p,a,x) = p\sqrt{\pi a}\, G(x)$$

where G(x) is the Green's function representing the geometry factor of the crack geometry under a unit of point loads on crack faces. The stress intensity factor solution for the problem in Figure 8(a) can be calculated as

$$K(p,a) = \int_0^a \Delta K(p,a,x)\,dx$$

For the stress gradient $\sigma(x) = \sigma_0\,\phi(x)$ as shown in Figure 8(a), the load per unit thickness at a distance x from the edge of the hole can be expressed by

$$p(x) = \sigma_0\,\phi(x)\,dx$$

Therefore, the stress intensity factor for the same geometry subjected to the stress gradient $\sigma(x) = \sigma_o\phi(x)$ on crack faces can be calculated as

$$K = \sigma_0\sqrt{\pi a}\int_0^a \phi(x)G(x)\,dx$$

The geometry factor β can be obtained as

$$\beta = K / K_o$$

where K_o is the stress intensity factor, i.e., $K_0 = \sigma_0\sqrt{\pi a}$.

Method 3: Compounding method

To account for the hole effect on the stress intensity factor of a crack at a hole growing toward an adjacent hole, an engineering approach by compounding the relevant geometry factors is employed. The method can be illustrated using an example.

Suppose the crack tip stress intensity factor of the geometry shown in Figure 9 is sought.

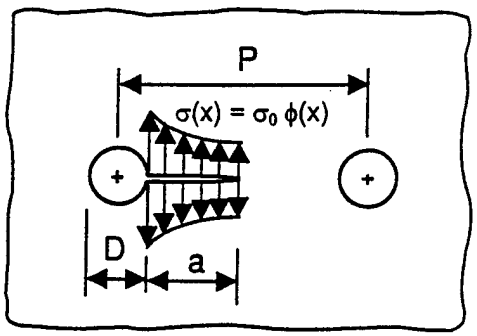

Figure 9. A Crack at a Hole Approaching an Adjacent Hole

The stress intensity factor can be estimated as

$$K = \sigma_0 \sqrt{\pi a}\, \beta_{Compound}$$

where $\beta_{Com[pound}$ is the compounded geometry factor calculated as the product of the geometry factors $\beta_{At\ a\ Hole}$ and $\beta_{Approaching\ a\ Hole}$, i.e.,

$$\beta_{Compounded} = \beta_{At\ a\ Hole} \times \beta_{Approaching\ a\ Hole}$$

For the case of a crack emanating from a hole in a wide plate subjected to stress gradients on crack faces as shown in Figure 10, the geometry factor $\beta_{At\ a\ Hole}$ can be obtained using the weight function method described in Method 2. For the case of a crack growing toward a hole, the geometry factors $\beta_{Approaching\ a\ Hole}$ are obtained from an open literature and are presented in Figure 11.

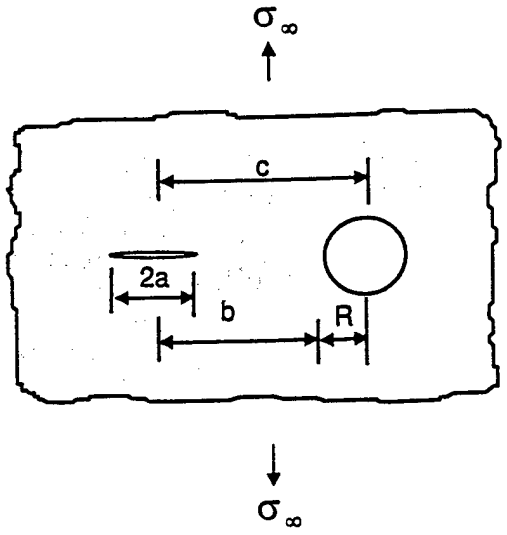

Figure 10. A Crack Approaching a Hole

$$K_o = \sigma_\infty \sqrt{\pi a}$$

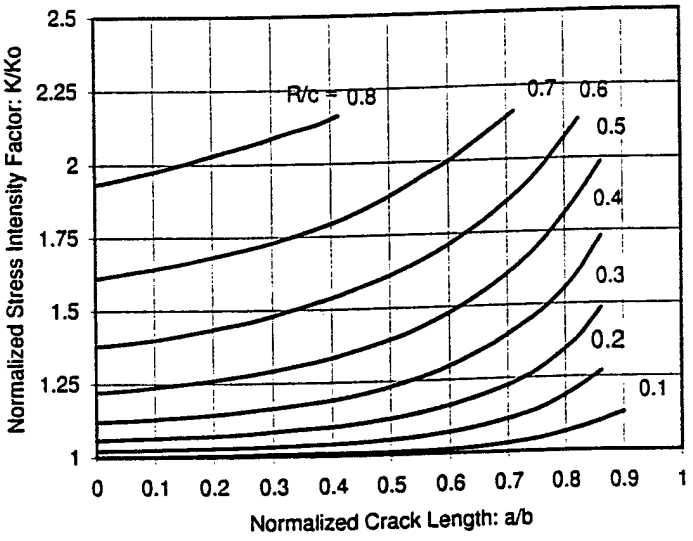

Figure 11. Geometry Factors for a Crack Approaching a Hole

3.5 Residual Strength Evaluation and Limit Stress

3.5.1 Fracture Toughness Method

The residual strength of the modified skin for antenna installation is calculated using the fracture toughness method

$$\sigma_{Residual} = \frac{K_C}{\beta\sqrt{\pi a}}$$

where K_C is the toughness of the skin material, β is the geometry factor, and a denotes the crack length. For small crack lengths, the residual strength is determined using the Fedderson's method. In this method, a tangent line from the yield stress σ_y of the material to the residual strength curve obtained using the fracture toughness method is numerically obtained as illustrated below in Figure 12.

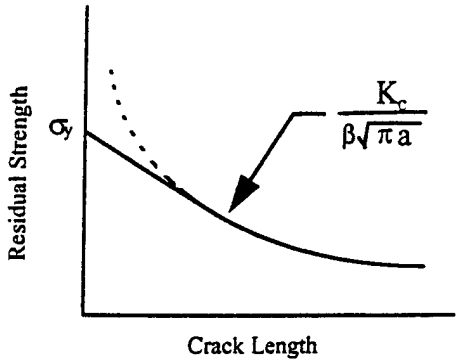

Figure 12. Residual Strength Curve

3.5.2 Limit Stresses

To assess the residual strength capability of the modified skin, the residual strength calculated in Section 3.5.1 is checked against the limit stress of the skin. In the analysis, the crack continues to grow until the residual strength of the skin is no longer greater than the limit stress.

The limit stress in the circumferential direction, for the longitudinal crack, is calculated using the equation

$$\sigma_{Limit,Circumferential} = 1.1\frac{pR}{t} + 0.6\frac{R}{t}$$

where p is the pressure differential, R and t are the radius and thickness of the fuselage shell at the location where the damage tolerance analysis is performed. The stress due to the additional pressure 0.6 psi in the equation is to account for the external aerodynamic suction pressure (0.5 psi) plus a 0.1 psi regulator tolerance per FAR 23.574.

The limit stress in the longitudinal direction, for the circumferential crack, is determined using the equation

$$\sigma_{Limit,Longitudinal} = \frac{pR}{2t} + 0.6\frac{R}{2t} + n_1 \sigma_{1G} / \gamma$$

where p is the pressure differential, n_1 is the maneuvering limit load factor, γ is the payload reduction factor, R and t are the radius and thickness of the fuselage shell, and σ_{1G} is the one-G stress at the location where the damage tolerance analysis is performed. The additional pressure 0.6 psi is added per FAR 23.574.

3.6 Load/Stress Spectrum and Equivalent Stress

To perform the cycle-by-cycle crack growth analysis of a modified skin to antenna installation, the stress spectrum that exerts on the skin needs to be prescribed. The stress spectrum is generally derived from the airplane C.G. load spectrum which is developed from the airplane flight profiles, exceedance data, and pressure schedule. The procedures of load and stress spectra development for commuter airplanes are described in Appendix B.

In RAPIDC, the stress spectrum can be converted into a constant amplitude stress spectrum representing a single cycle of an equivalent repeated flight. The constant amplitude stress spectrum is then used in the simplified crack growth analysis. The procedure is described in Appendix C.

3.7 Crack Growth Rate Data

The crack growth da/dN vs. ΔK data are obtained experimentally from constant amplitude coupon tests for the material, and are normally documented in a tabular or graphic form. The tabulated data can be used directly in the crack growth calculation using the cycle-by-cycle method. To use the simplified method, the tabular data need to be curve-fitted to the Walker's equation:

$$\frac{da}{dN} = C\left[(1-R)^q K_{max}\right]^p$$

In RAPIDC, the following da/dN versus ΔK tabular data as well as the coefficients C, p, and q in the Walker's equation of thirteen materials are included in the material database.

(1) 2024-T3 Clad Sheet, -T42 Bare Sheet, L-T RT LA DW
(2) 2024-T3 Clad Sheet, -T42 Bare Sheet, T-L RT LA DW
(3) 2024-T351 Plate, -T3511 Extrusion, L-T RT LA DW
(4) 7050-T7452 Forging, L-T T-L LA RT
(5) 7050-T74511, -T76511 Extrusion, L-T RT LA DW
(6) 7050-T74511 Extrusion, L-T RT STW
(7) 7050-T7651, -T7451 Plate, L-T T-L RT LA DW

(8) 7050-T76511 Extrusion, L-T RT STW
(9) 7475-T7351 Plate, L-T LA RT
(10) 7475-T7651 Plate, L-T LA RT DW
(11) 7475-T761 Clad Sheet, L-T RT LA DW
(12) 7075-T6 Clad Sheet, L-T RT LA
(13) 2014-T6 Sheet, T=0.05 L-T RT LA 10 HZ

where

L-T: longitudinal-transverse material orientation
T-L: transverse-longitudinal material orientation
RT: room temperature test condition
LA: laboratory air environmental test condition
DW: distilled water environmental test condition
STW: sump tank water environmental test condition

RAPIDC also provides user with a direct input of da/dN tabular data or Walker's coefficients. The input format of the da/dN tabular data is described as follows.

Line 1→	1							
	3	30	(2024-T3 CLAD SHEET,-T42 BARE SHEET, L-T RT LA DW)					
		0.05	0.40	0.80				
Line 4 →	0.100E-31	0.100E-07	0.300E-07	0.500E-07	0.700E-07	0.800E-07	0.100E-06	0.200E-06
	0.300E-06	0.500E-06	0.800E-06	0.100E-05	0.200E-05	0.500E-05	0.800E-05	0.100E-04
	0.200E-04	0.400E-04	0.800E-04	0.100E-03	0.200E-03	0.500E-03	0.100E-02	0.300E-02
	0.800E-02	0.200E-01	0.500E-01	0.100E+00	0.200E+00	0.100E+01		
Line →	2.8990	2.9000	2.9010	3.0000	3.2000	3.3000	3.6000	4.7500
	5.5000	6.2000	6.6000	6.8000	8.0000	10.1000	12.2000	13.2500
	16.9000	20.0000	24.2000	25.6000	29.6000	36.0000	41.0000	50.5000
	61.0000	70.0000	78.0000	87.0000	92.0000	93.0000		
Line 12→	2.3480	2.3490	2.3500	2.3600	2.5000	2.6000	2.8800	3.9000
	4.5000	5.1500	5.7000	6.0000	7.0000	8.7500	9.9000	10.5000
	13.2500	16.0000	19.5000	21.0000	24.5000	29.0000	33.5000	41.5000
	48.0000	51.0000	54.0000	56.5000	57.0000	58.0000		
Line 16→	1.7490	1.7500	1.7600	1.7700	1.8200	1.8750	2.0500	2.8500
	3.4000	4.0000	4.5000	4.8000	5.6000	7.0000	8.0000	8.4000
	9.9000	11.5000	13.0000	13.5000	15.3000	18.0000	19.8000	20.0000
	20.0010	20.0020	20.0030	20.0040	20.0050	20.0060		

Line	Acronym	Type	Definition
1	NMAT	Integer	The material number that corresponds with the material number containing the Walker's C, p and q values
2	MRATIO	Integer	The first integer number is the number of different ratio values in line 3; the maximum value is 10
2	MVALUE	Integer	The second integer value is the number of da/dN values in lines 4-7, and ΔK values in lines 8-11, 12-15, and 16-19; the maximum value is 40
2	-	-	Description of the material; optional
3	RATIOV	Real	The different ratio values in ascending order; there are *MRATIO* values
4-7	DADN	Real	The da/dN values; there are *MVALUE* values for this y-axis
8-11, 12-15, 16-19	DELTAK	Real	The ΔK values; there are *MVALUE* values, and *MRATIO* sets for this x-axis

3.8 Crack Growth Analysis

Two methods, the simplified method and the cycle-by-cycle method, are implemented in RAPIDC to calculate the crack growth life of the modified skin.

3.8.1 Simplified Method

The crack growth of a cracked skin can be calculated using the simplified method based on the Walker's crack growth equation. The number of flights N_{ij} for a crack growing from the size a_i to the size a_j ($a_j > a_i$) is calculated as

$$N_{ij} = \frac{1}{C}(SG_{ij})^{-p}$$

where S is the one cycle equivalent stress, C and p are the coefficients in Walker's equation, and the geometry term G_{ij}^{-p} can be calculated as

$$G_{ij}^{-p} = \int_{a_i}^{a_j} [\beta(a)\sqrt{\pi a}]^{-p}\, da$$

Let the integrand in the above integral be represented by the geometric function g(a), i.e.,

$$g(a) = [\beta(a)\sqrt{\pi a}]^{-p}$$

where $\beta(a)$ is the compounded normalized stress intensity factor obtained as

$$\beta(a) = \beta_{\text{AtorPassingThroughHole(s)}}\, \beta_{\text{ApproachingHole}}$$

The terms $\beta_{\text{At or Passing Through Hole(s)}}$ and $\beta_{\text{Approaching Hole}}$ are the geometry factors of relevant crack configurations as described in Sections 3.4.

The integral of the geometric function represents the geometry terms. Since the geometry factors are normally presented in a tabular form, the integral is carried out numerically using the Gaussian Quadrature method.

In the Gaussian Quadrature method, the integral can be approximated by the following equation:

$$G_{ij}^{-p} = \frac{a_j - a_i}{2} \sum_{k=1}^{K} w_k\, g(a_k)$$

where

$$g(a_k) = [\beta(a_k)\sqrt{\pi a_k}\,]^{-p}$$

and

$$a_k = \frac{(a_j - a_i)\, t_k + (a_j + a_i)}{2}$$

In the above equations, the variables w_k and t_k are the k-th weighting coefficient and root of the K-th order Legendre polynomial $P_K(t) = 0$. For instance, numerical values of w and t for the case of K = 4 are given below.

k	W_k	t_k
1	0.347855	-0.861136
2	0.652145	-0.339981
3	0.652145	0.339981
4	0.347855	0.861136

It is noted that the simplified method calculates the number of flights N_{ij} for a crack growing from a size a_i to a next size a_j ($a_j > a_i$). With this method, the number of flights can be calculated in one step for a crack growing from an initial size to the final size. To generate crack growth life at intermediate crack lengths, the procedure is carried out between two crack lengths and iterated to complete the crack growth analysis.

3.8.2 Cycle-by-Cycle Method

The cycle-by-cycle crack growth analysis method is illustrated using an example as shown in figure13. A flow chart of the analysis procedure is provided in Figure 14.

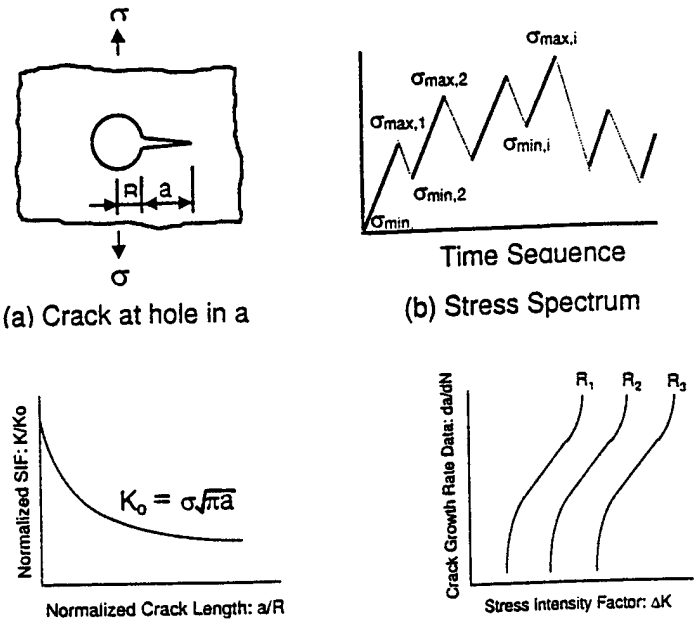

(a) Crack at hole in a

(b) Stress Spectrum

Figure 13. Description of Crack Growth Analysis Method

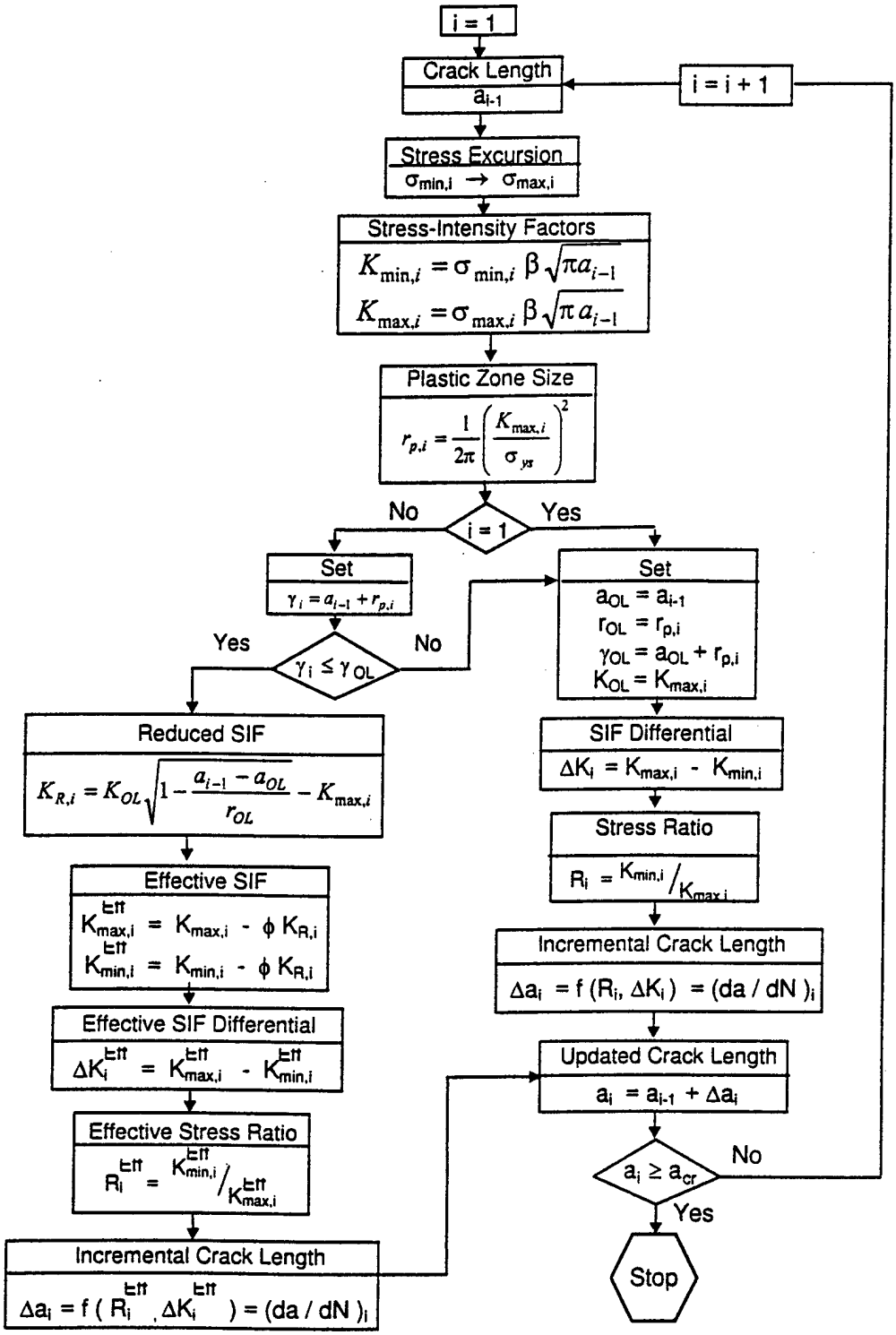

Figure 14. Flow Chart of the Cycle-by-Cycle Crack Growth Analysis

Let a_0 be the initial crack length. The crack growth analysis starts with an initial crack of length a_0 at i = 1. For the first cycle stress excursion, the stress-intensity factor and the plastic zone size are calculated. With the stress ratio R and the

change of the stress-intensity factor ΔK, the incremental crack length is obtained from the da/dN data. The crack is incremented to the length a_1.

At each sequential i-th cycle, the crack growth starts with a length equal to a_{i-1}. The stress-intensity factor and the plastic zone size are calculated using the i-th stress excursion. A test is then made to determine if the growth of the progressing crack is retarded. A positive answer leads the analysis to use the Generalized Willenborg retardation model in the calculation of incremental crack length. Otherwise, the retardation effect is bypassed in the calculation. During the i-th cycle, the crack advances a length of Δa_i and grows to a length $a_i = a_{i-1} + \Delta a_i$.

The process continues until the crack grows to the critical crack length determined from the residual strength analysis.

In the analysis, the compression-tension stress cycle is treated as a zero-tension stress cycle and the compression-compression stress cycle is ignored in the crack growth calculation. Furthermore, the parameter ϕ introduced in the generalized Willenborg retardation model to calculate the effective stress intensity factor (see flowchart in Figure 14) is calculated by the equation

$$\phi = \frac{1 - \frac{\Delta K_{Threshold}}{\Delta K_i}}{S^{OL} - 1}$$

where $\Delta K_{Threshold}$ is the threshold stress-intensity factor level associated with zero fatigue crack growth rates, and S^{OL} is the overload (shut-off) ratio required to cause crack arrest for the given material. A value of 2.3 is used in RAPIDC.

4.0 Inspection Threshold and Interval

With the crack growth life of the modified skin provided by RAPIDC, the user determines the inspection threshold and the inspection interval at the detectable crack length for the desired inspection method.

5.0 Example Problem

The damage tolerance analysis of a modified skin to an antenna installation is performed below for three crack scenarios described in Section 3.3.

Description of the Example Problem

Figure 15 depicts an example problem of an antenna installation on the fuselage of a commuter airplane. Assume that the skin is subjected to an equivalent one cycle circumferential stress of 18 ksi with zero stress ratio. Damage tolerance

analysis of the modified skin is carried out to demonstrate the analysis procedure.

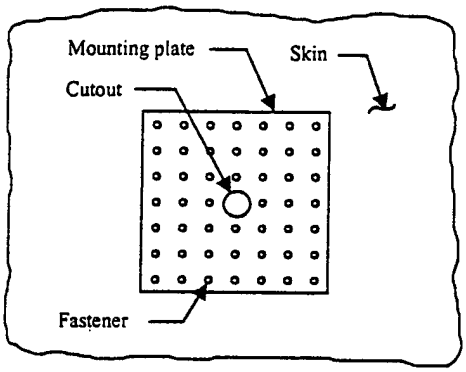

Fuselage radius: 60.0"
Skin thickness: 0.050"
Mounting plate thickness: 0.063"
Cutout diameter: 1.0"
Fastener diameter: 3/16"
Fastener rows: 3
Fastener pitch: 1.0"
Skin and mounting plate: Al2024T3
Fastener: NAS1097
Fracture toughness: 153 ksi sqrt(in)
Pressure differential: 8.6 psi

Figure 15. Description of the Example Problem

Fastener Loads and Stress Gradients

(1) Fastener Loads

Figure 16 shows load transfers at fasteners in pounds due to 1000 psi reference skin stress. These fastener loads were obtained using FRANC2DL as described in Appendix A. As expected, the outer row is the critical fastener row.

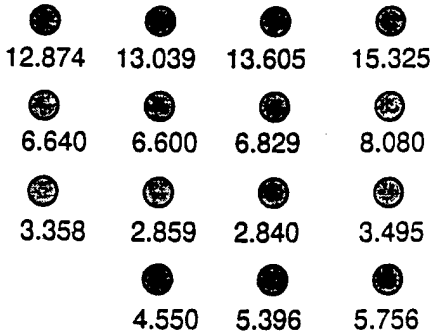

Figure 16. Fastener Loads

2. Stress Gradients

The crack growth scenario 3 described in Section 3.3 is depicted in Figure 17.

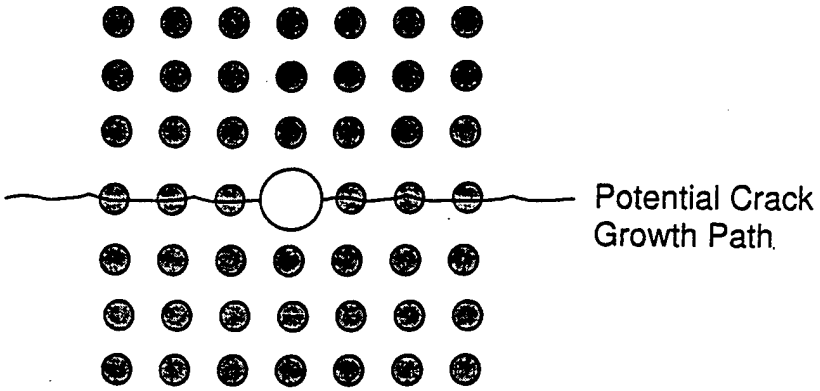

Figure 17. Potential Crack Growth Paths

The stress gradient along the potential crack path subjected to 1,000 psi reference skin stress is shown in Figure 18. The distance d is measured from the center of the hole.

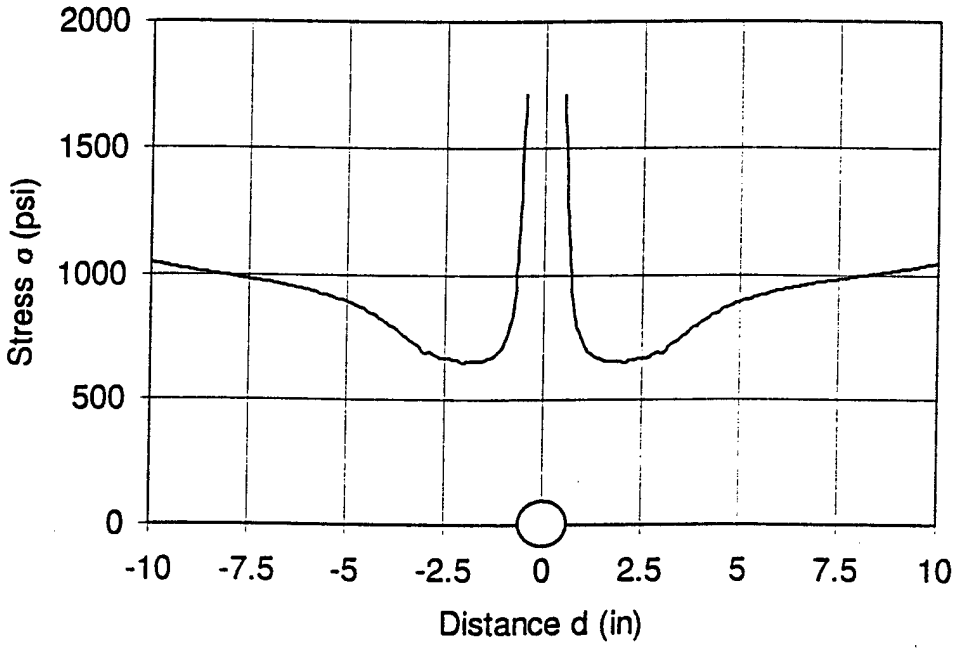

Figure 18. Stress Gradient along Potential Crack Growth Path

Residual Strength and Crack Growth

To demonstrate the residual strength and crack growth analysis of the example problem, analysis is performed for three Scenarios described in Section 3.3.

(1) Stress Intensity Factors

Stress intensity factors for a crack initiating from the center or the corner fastener hole due to gross, bearing, and bypass stresses are calculated using the superposition method. The effect of a crack growing toward an adjacent hole is accounted for using the compounding method.

For a crack initiating from the antenna connector hole, the weight function method is used. Using the stress gradients shown in Figure 18, the normalized stress intensity factor or geometry factor is obtained as shown in Figure 19.

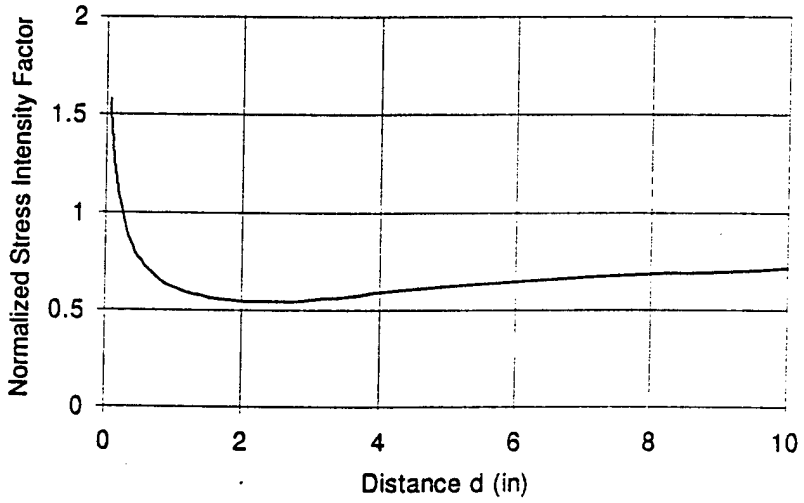

Figure 19. Normalized Stress Intensity Factors

The effect of a crack growing toward an adjacent hole is accounted for using the compounding method.

(2) Residual Strength

Residual strengths of the skin are calculated using the fracture toughness method and modified using Fedderson's criterion. The calculation terminates when the residual strength reaches the limit stress of 12,072 psi obtained using the circumferential limit stress equation in Section 3.5.2. Figure 20 shows the residual strength curve.

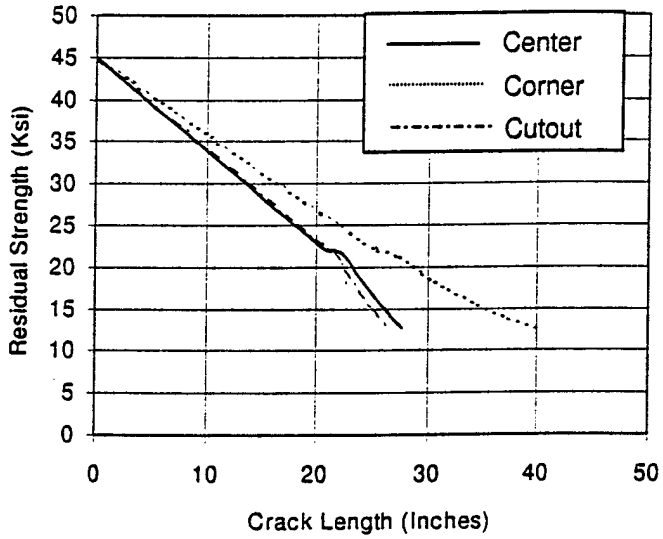

Figure 20. Residual Strength

(3) Crack Growth Lives

Figure 21 shows the crack growth lives obtained using the simplified crack growth analysis method.

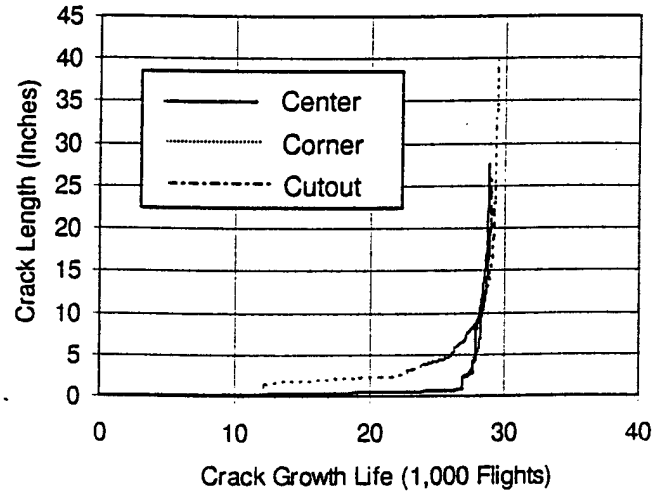

Figure 21. Crack Growth Life

Inspection Threshold and Interval

Once the residual strength and crack growth life have been obtained, the critical crack length can be determined from the residual strength at the limit stress. The crack growth life at the critical crack length can then be determined from the crack growth life curve.

With the crack growth history, the inspection threshold and interval can be determined from the crack growth life based on the detectable crack size of the inspection method.

Appendix A

Fastener Loads and Skin Stress Gradients Calculations

A1. Introduction

This appendix describes the database development of load transfers along the critical outermost fastener row and stress gradients along the potential crack growth path, for a flaw initiating from the antenna connector hole, normal to the stress application direction in a modified skin to antenna installation. The purpose of the work is to determine fastener loads and stress gradients required in the calculation of stress intensity factor for the damage tolerance analysis. The database is developed for square/rectangular and circular antenna installations typically found in commuter airplanes. A similar database will be developed for elliptical installations in the next phase of contract.

A2. Types of Antenna Installation

Three types of antenna installation are common on the fuselage skin of commuter airplanes. Typical mounting plates in most antenna installations including rectangular, circular, and elliptical shapes are shown in Figure A1. In all installations, the mounting plate is mechanically fastened to the skin around the antenna connector hole cutout.

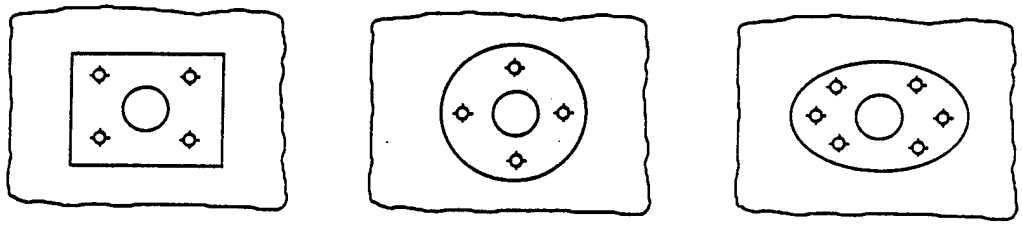

(a) Rectangular (b) Circular (c) Elliptical

Figure A1. Three types of antenna installation

In RAPIDC Version 1.0, only the circular and square/rectangular installations are considered. The elliptical installations will be included in the next phase of contract.

A3. Approach

To perform the damage tolerance analysis, fastener loads or skin stress gradients along the potential crack growth path are needed when calculating crack tip stress intensity factors. The determination of fastener loads and skin stress gradients can be accomplished using the FRANC2D/L program developed jointly at Cornell University and Kansas State University sponsored by NASA-

Langley Research center. The finite element model can be created using the FRANC2D/L preprocessor program called CASCA developed at Cornell University. Figure A2 shows a typical finite element model representing one quarter of the modified skin and a mounting plate attached to the skin created using the CASCA program. In the figure, the triangle symbol indicates the fastener location and the heavy solid line represents the boundary of the mounting plate. In the analysis, the skin is subjected to a uniform far field stress applied along the top boundary. Due to double symmetry of the geometry as well as the loading, translational displacements are constrained along the left and bottom edges of the model (both skin and mounting plate) in the analysis.

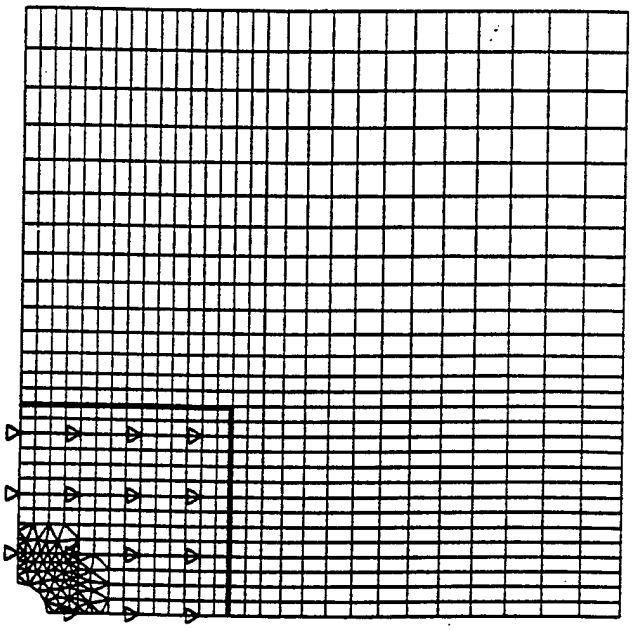

Figure A2. Finite Element of One Quarter of the Modified Skin with Mounting Plate and Fasteners

In FRANC2D/L analysis, the fastener shear rigidity needs to be calculated separately and input into the program. The FRANC2D/L assembles the stiffness contributing from each of the structural components, skin, mounting plate and fasteners, to form an overall stiffness matrix. With the loads applied to the structural model, FRANC2D/L solves for deformations, load transfers, and stress in the skin and mounting plate.

The shear rigidity of the fastener can be calculated using the Swift's empirical equation:

$$K = \frac{E\,d}{A + B\left(\frac{d}{t_{Skin}} + \frac{d}{t_{MountingPlate}}\right)}$$

where E is the weighted Young's modules of the skin and mounting plate, d is the fastener hole diameter, t_{Skin} and $t_{Mounting\ Plate}$ are the thickness of the skin and mounting plate, respectively, and A and B are material dependent empirical constants. The values of A and B, for aluminum fasteners, are 5.0 and 0.8, respectively.

In the analysis, a reference uniform far field stress of 1,000 psi is applied along the top edge of the model.

A4. Parameters

Parameters considered in the fastener loads and skin stress gradients calculations for square/rectangular and circular installations include:

Skin thickness: 0.032", 0.040", 0.050", and 0.063"
Mounting plate thickness: 1 gauge higher than skin thickness
Antenna connector hole diameter: 1.0", 2.0", and 3.0"
Fastener size: 1/8", 5/32", and 3/16"
Number of fastener rows: 1 ~ 5 on each side
Aspect ratio: 1:1 (square), 1:1.3 and 1:1.6
Materials: Aluminum skin and mounting plate
Aluminum fastener

In the database development, the number of fastener rows, in rectangular installations, normal to the stress application direction is limited to 3 on each side. However, it is limited to 5 on each side for the fastener rows parallel to the stress application direction. For circular installations, the number of fastener rings is limited to 3.

A total of 180 rectangular and 108 circular antenna installations are included in the fastener loads and skin stress gradients database.

A5. Results

Analysis results of fastener loads along the critical outmost faster row are obtained based on a 1,000 psi reference skin stress for 180 rectangular and 108 circular antenna installations. These fastener loads are used to calculate the bearing and bypass stresses which are used in the stress intensity factor calculation. Stress gradients along a crack growth path normal to the stress application direction are also obtained for a crack initiating from the antenna connector hole. These stress gradients are used in the stress intensity factor calculation.

A6. Examples

Figure A3 depicts an example problem of an antenna installation on the fuselage of a commuter airplane.

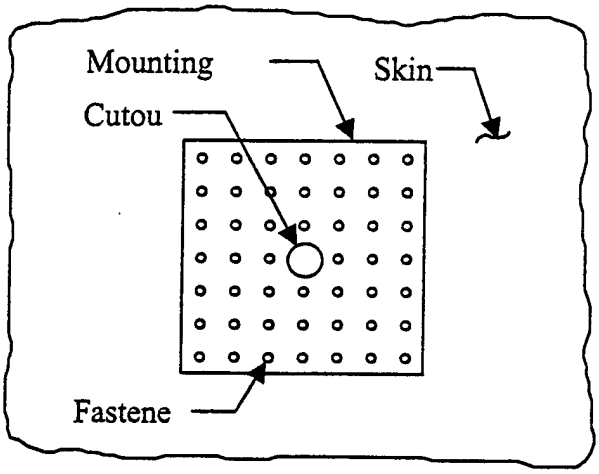

Skin thickness: 0.050"
Mounting plate thickness: 0.063"
Cutout diameter: 1.0"
Fastener diameter: 3/16"
Fastener rows: 3 on each side
Fastener pitch: 1.0"
Skin and mounting plate: Al2024T3
Fastener: NAS1097

Figure A3. Description of the Example Problem

Fastener loads in pounds obtained from FRANC2DL are shown in Figure A4. It shows that load transfers at fasteners along the outermost row are larger than other rows.

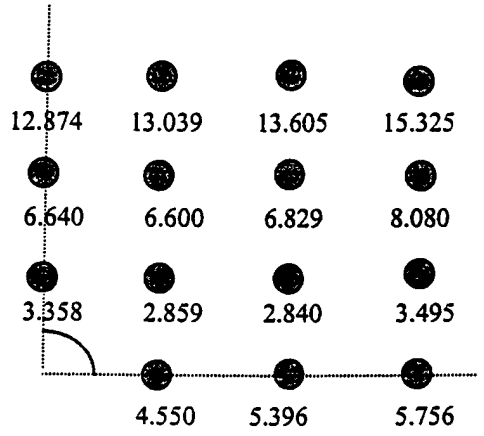

Figure A4. Fastener Loads

One of the initial flaw assumptions in an antenna installation is to postulate an initial crack at the antenna connector hole. With this assumption, the crack continues to grow along a path normal to the stress application direction as shown in Figure A5.

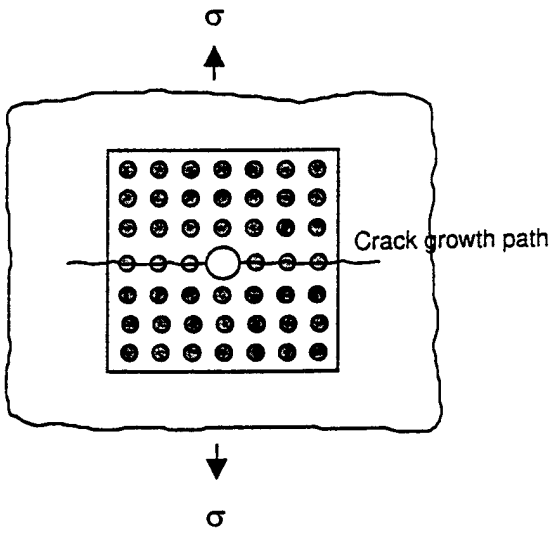

Figure A5. Potential Crack Growth Paths

The stress gradient along the potential crack growth path is shown in Figure A6. The distance d shown in the figure is measured from the center of the hole. This stress gradient is used in the stress intensity factor calculation for damage tolerance analysis.

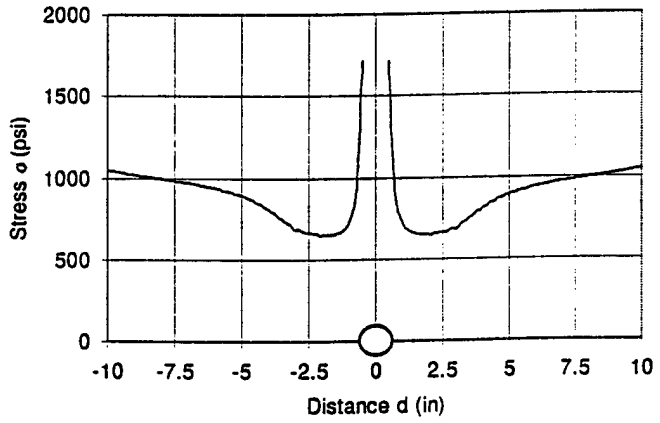

Figure A6. Stress Gradient along Potential Crack Growth Path

Appendix B

Load/Stress Spectrum Development

B1. Introduction

This Appendix describes procedures used in RAPIDC to develop the load spectrum at the airplane C.G. location for commuter airplanes. The load spectrum consists of load sequences that an airplane experiences in a flight including pre-flight taxi, climbing, cruise, descending, landing impact, and post-flight taxi. To perform the damage tolerance analysis of a structural component on an airplane, a stress spectrum is required. In RAPIDC, a simple method based on the material allowable is used to derive the stress spectrum from the load spectrum.

The steps taken to generate load and stress spectra in RAPIDC are outlined below.

1 User provides RAPIDC with characteristics of the airplane such as the design maximum take-off weight, the wing surface area, the maximum design cruise altitude, and the normal maximum working pressure.

2 User provides RAPIDC with up to six airplane usage data such as the flight distances, the cruise altitude, and the cruise speed.

3 Incorporate maneuver and gust exceedance data from DOT/FAA/CT-91/20 (Reference 1) for single and twin engine pressurized general usage into RAPIDC.

4 Randomize flight profile mixes to create load sequences for each flight segment and form a complete flight load spectrum.

5 Derive the stress spectra at the location of interest from the load spectrum based on the skin material allowable.

The load spectrum created for RAPIDC consists of 3,000 flights of load sequences in terms of the change of airplane C.G. normal acceleration (Δg) from the 1-G flight. RAPIDC creates a load sequence of one tenth of the airplane design life when the user optionally provides RAPIDC with the design life of the airplane.

B2. Input Parameters Required for Load and Stress Spectra development

To generate the load spectrum, the user is required to provide RAPIDC with the following data:

1. Airplane design maximum take-off weight (lbs)
2. Nominal maximum working pressure (psi)
3. Flight distance (statue or nautical miles)
4. Maximum design cruise altitude (feet)
5. Cruise speed (KEAS)
6. Cruise altitude (feet)
7. Wing surface area (feet^2)
8. Airplane design life (flights)

The following additional pieces of information are also required to derive the stress spectrum from the load spectrum.

1. Fuselage radius at the location of interest
2. Zone number indicating the location of interest (see Figure B1)
3. Zone Length (S)
4. Distance between zone starting point and the location of interest (L)
5. Distance between cabin floor and the location of interest (Z)

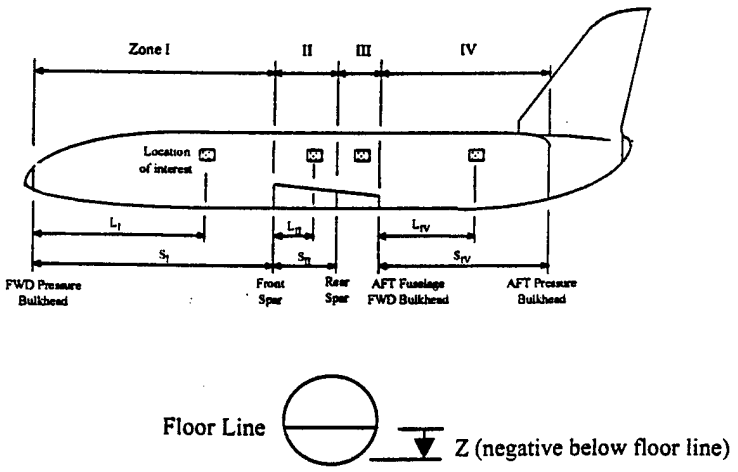

Figure B1. Airplane Zones

B3. Flight Profiles

A typical flight profile of commuter airplanes can be divided into stages of operation. The time line of the operation stages is schematically shown in Figure B2 and the stages used in the RAPIDC program and the load environments are described in Table B1. RAPIDC accepts up to six flight profiles provided by the user. A randomized mission mix scheme is used to generate the load spectrum.

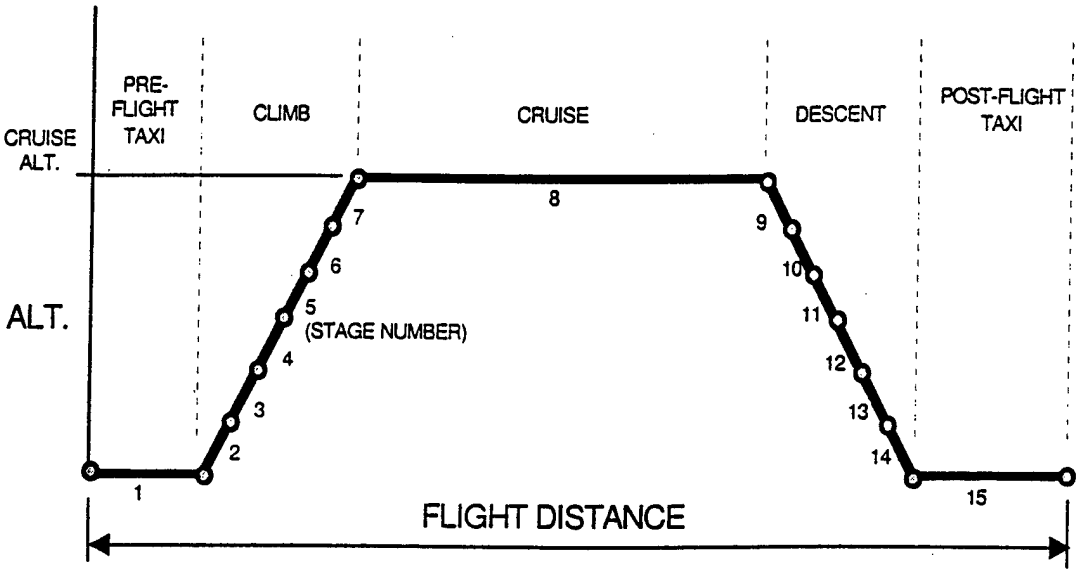

Figure B2. Typical Flight Profile

Table B1. Flight Segments

Stage No	Stage	Load Environment
1	Pre-flight Taxi	Ground
2-7	Climb	Gust and Maneuver
8	Cruise	Gust and Maneuver
9-14	Descent	Gust and Maneuver
15	Post-flight Taxi	Ground

B3.1 Assumptions

To construct a flight profile, the following assumptions are made:

1 There are six climbing stages and six descending stages for a flight profile.

2 For a flight profile, the duration for climb and descent is each determined linearly using three baseline flight duration data.

3 The airplane equivalent speed increases linearly in proportion to the altitude from the time of takeoff (zero speed) to the beginning of cruise. Similarly, it decreases linearly from cruise to landing (zero speed) during descent.

The three baseline flight duration data in RAPIDC are defined as follows.

Baseline 1:

Flight duration = 30 minutes
Climb and descent duration = 6 minutes each

Baseline 2:

Flight duration = 60 minutes
Climb and descent duration = 8 minutes each

Baseline 3:

Flight duration = 120 minutes
Climb and descent duration = 10 minutes each

B3.2 Construction of Flight Profile

The following steps are used to construct a flight profile:

1 Compute the altitude for the climbing stages which is linearly interpolated based on the altitude at the ground zero level and that at the cruise altitude.

2 Compute the altitude for the descending stages which is linearly interpolated based on the altitude at the cruise altitude and ground zero level.

3 Compute average speed for the climbing stages which is linearly interpolated based on the equivalent speed at takeoff and that at cruise as a function of airplane altitude.

4 Compute average speed for the descending stages which is linearly interpolated based on the equivalent speed at cruise and that at landing as a function of airplane altitude.

5 Compute the duration for the climbing stages which is linearly interpolated using three baseline flight duration data.

6 Compute the duration for the descending stages which is linearly interpolated using three baseline flight duration data.

7 Compute the cabin pressure at each stage as a function of altitude from the pressure schedule described in Section B4.1.4.

B3.3 An Example: Flight Profile

Table 2 gives parameters used to create a flight profile for a typical commuter airplane.

Table B2. Operation Parameter Profile for a Typical Commuter Airplane

Airplane Parameters	Units	Typical Commuter Airplane
Flight Distance	st. miles	204
Design Maximum Takeoff Weight	lb.	16300
Wing Area	ft^2	310
Cruise Altitude	ft.	35,000
Maximum Cruise Altitude	ft.	45000
Nominal Maximum Working Pressure	psi	9.3
Cruise Speed	KEAS	240
Climb Duration	hrs.	0.12834
Descent Duration	hrs.	0.12834

The flight profile generated from above operation parameters is shown in Table B3.

Table 3. A Typical flight Profile for Commuter airplanes

Segment Number	Altitude (1000 Ft.)	Speed (KEAS)	Duration (Hours)	Cabin Pressure (psi)
1	0	0.0	0.0	0.60
2	0-5.83	20.0	0.02139	2.04
3	5.83-11.67	60.0	0.02139	4.43
4	11.67-17.50	100.0	0.02139	6.28
5	17.50-23.33	140.0	0.02139	7.67
6	23.33-29.17	180.0	0.02139	8.68
7	29.17-35.0	220.0	0.02139	9.35
8	35	240.0	0.59330	9.59
9	35-29.17	220.0	0.02139	9.35
10	29.17-23.33	180.0	0.02139	8.68
11	23.33-17.50	140.0	0.02139	7.67
12	17.50-11.67	100.0	0.02139	6.28
13	11.67-5.83	60.0	0.02139	4.43
14	5.83-0	20.0	0.02139	2.04
15	0	0.0	0.0	0.60

B4. Load Spectrum at Airplane Center-of-Gravity

This section describes procedures of load sequence generation at the airplane C.G. location.

B4.1 Load Environments

Load environments contributing to the crack growth of a modified skin include the following:

1 In-flight maneuver operations during climb, cruise, descent and landing impact

2 Gust loads due to air turbulence

3 Ground operations such as pre-flight taxi and post-flight taxi

4 Cabin pressure

The frequency distribution of the accelerations that the airplane experiences at the center of gravity can be expressed in tabulated forms such as the load exceedance tables. These exceedance data are obtained from the FAA document (Reference 1) for general aviation aircraft. The acceleration exceedance data for each load environment are presented as follows.

B4.1.1 In-flight Maneuver

The distributions of airplane acceleration during climb, cruise, descent and landing impact for single and twin-engine pressurized general usage airplanes are shown in Figure B3. Shown in the figure are the cumulative frequency of exceedance or cumulative number of occurrences per nautical mile as a function of acceleration fraction $a_n/a_{n,LLF}$ where, a_n is the change of normal acceleration in the unit of g's and $a_{n,LLF}$ is the change of limit load factor.

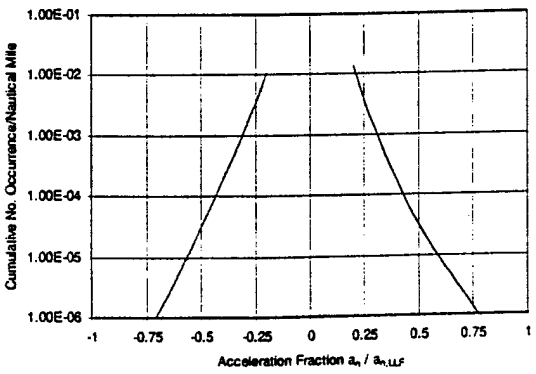

Figure B3. Maneuver Exceedance Data

It is noted that the above exceedance data are the cumulative number of occurrences per nautical mile. Load spectra, however, are generally expressed in terms of cycles per 1,000 flights. For this reason, the exceedance or the cumulative number of occurrences per nautical mile needs to be converted to that per 1,000 flights. This conversion is accomplished by multiplying the exceedance per nautical mile by the flight distance in nautical miles times 1,000 for 1,000 flights. To obtain the exceedance per spectrum, multiply the exceedance per 1,000 flights by the number of flights per spectrum (assuming 1/10 of the airplane design life, default to 3,000 flights) and then divided by 1,000 flights.

It should also be noted that the exceedance obtained from Reference 1 is tabulated in terms of acceleration fraction $a_n / a_{n,LLF}$. For practical use, the exceedance is expressed as a function of the change of normal acceleration a_n from the 1-G stress level. The conversion from the acceleration fraction $a_n / a_{n,LLF}$ to the change of normal acceleration a_n can be accomplished as follows.

For positive maneuver, the limit load factor n_1 is calculated as

$$n_1 = 2.1 + \frac{24{,}000}{W + 10{,}000}$$

where W is the design maximum take-off weight of the airplane in pounds. The calculated value of n_1 should be bounded between 2.5 and 3.8. The change of limit load factor $a_{n,LLF}$ is then calculated as

$$a_{n,LLF} = n_1 - 1.0$$

For negative maneuver, the limit load factor n_2 is calculated as

$$n_2 = -0.5\, n_1$$

The change of limit load factor $a_{n,LLF}$ is then calculated as

$$a_{n,LLF} = n_2 - 1.0$$

The change of acceleration a_n is then obtained by multiplying the acceleration fraction $a_n / a_{n,LLF}$ by the change of limit load factor $a_{n,LLF}$.

Figure B4 shows an example of the maneuver exceedance per 1,000 flights as a function of the change of normal acceleration for the operation parameters described in Table B2.

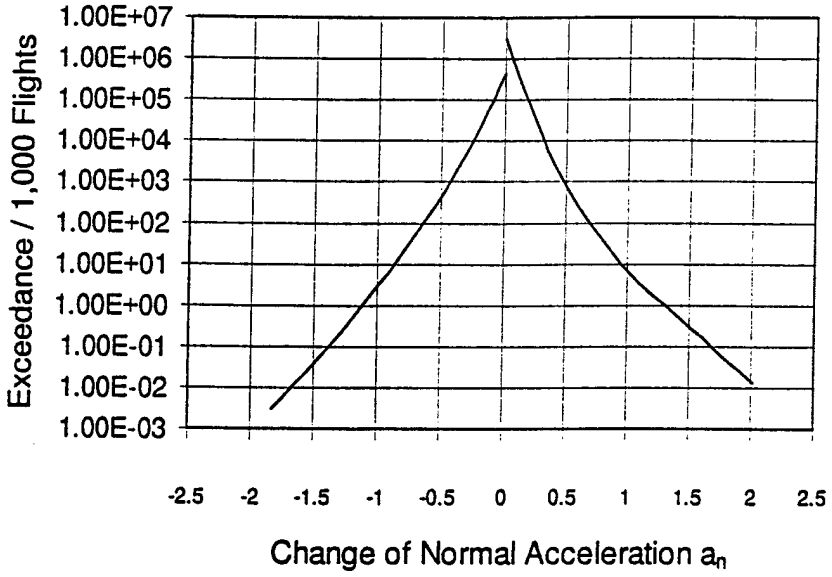

Figure B4. An Example of Maneuver Exceedance

B4.1.4 Gust

The distributions of airplane acceleration due to gust for single and twin-engine pressurized general usage airplanes are shown in Figure B5. Shown in the figure are the cumulative number of occurrences per nautical mile as a function of acceleration fraction $a_n/a_{n,LLF}$ where, a_n is the change of normal acceleration in the unit of g's and $a_{n,LLF}$ is the change of limit load factor.

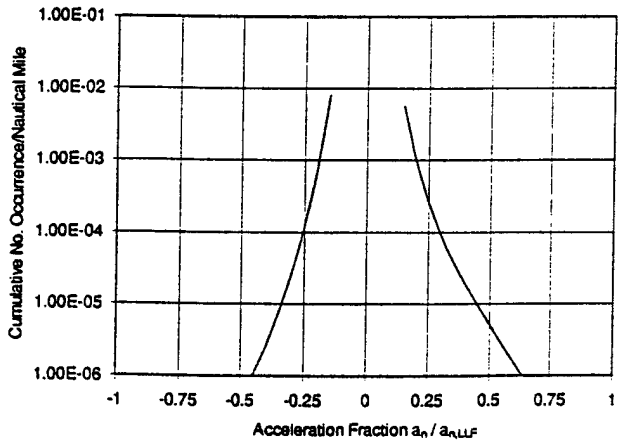

Figure B5. Gust Exceedance Data

The gust exceedance data obtained from Reference 1 are the cumulative occurrences per nautical mile in terms of the acceleration fraction. For the same reasons addressed in Section B4.1.2, the exceedance needs to be converted to cumulative occurrences per 1,000 flights as a function of the change of normal acceleration from the 1-G stress level. This can be accomplished using the same approach described in Section B4.1.2. However, the positive and negative gust limit load factors n_3 and n_4 as shown in Figures B6 and B7, respectively, should be used per FAR Part 23, Appendix A (Reference 2).

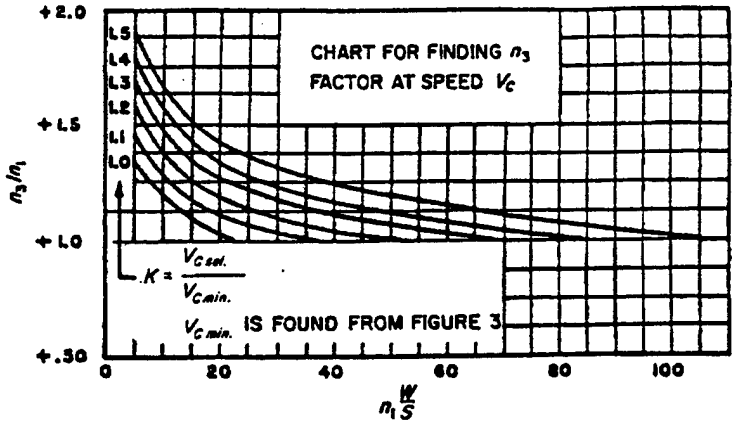

Figure B6. Determination of n_3 Factor at Speed V_c

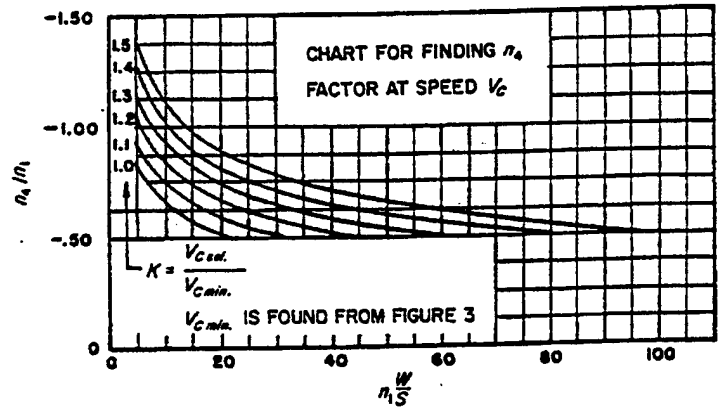

Figure B7. Determination of n_4 Factor at Speed V_c

In Figures B6 and B7, n_1 is the positive maneuver limit load factor, W is the design maximum take-off weight of the airplane (pounds), S is the airplane wing surface (feet^2), $V_{C,\,Sel}$ is the airplane cruise speed (KTAS), and $V_{C,Min}$ is the minimum design cruise speed (KTAS) which is calculated as

$$V_{C,Min} = 17.0\sqrt{n_1 \frac{W}{S}}$$

Once the positive and negative limit load factors n_3 and n_4 are obtained, the change of limit load factors can be calculated as

For positive gust exceedance

$$a_{n,LLF} = n_3 - 1.0$$

For negative gust exceedance

$$a_{n,LLF} = n_4 - 1.0$$

Figure B8 shows an example of the gust exceedance per 1,000 flights as a function of the change of normal acceleration for the operation parameters described in Table B2.

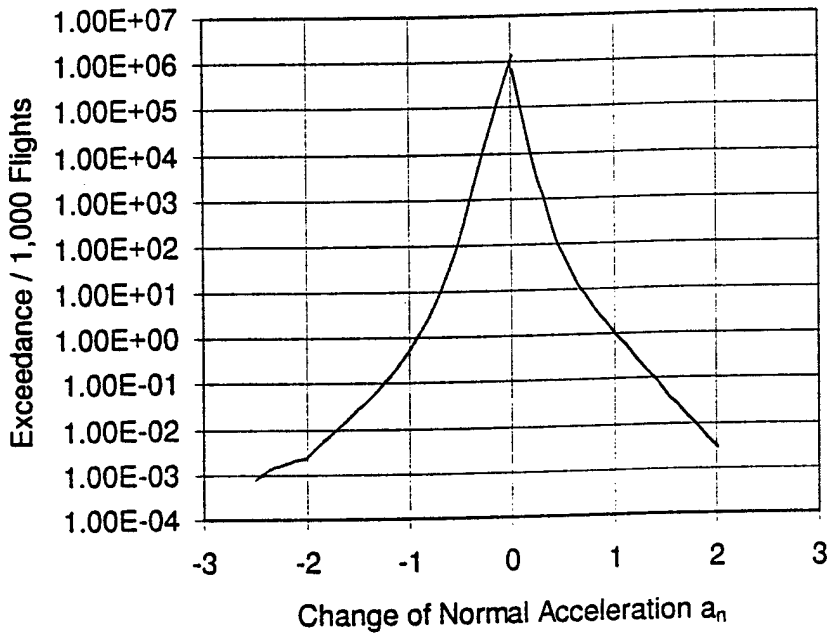

Figure B8. An Example of Gust Exceedance

B4.1.3 Taxi

The distributions of airplane acceleration during ground operations are shown in Figure B9 for 1,000 flight operations.

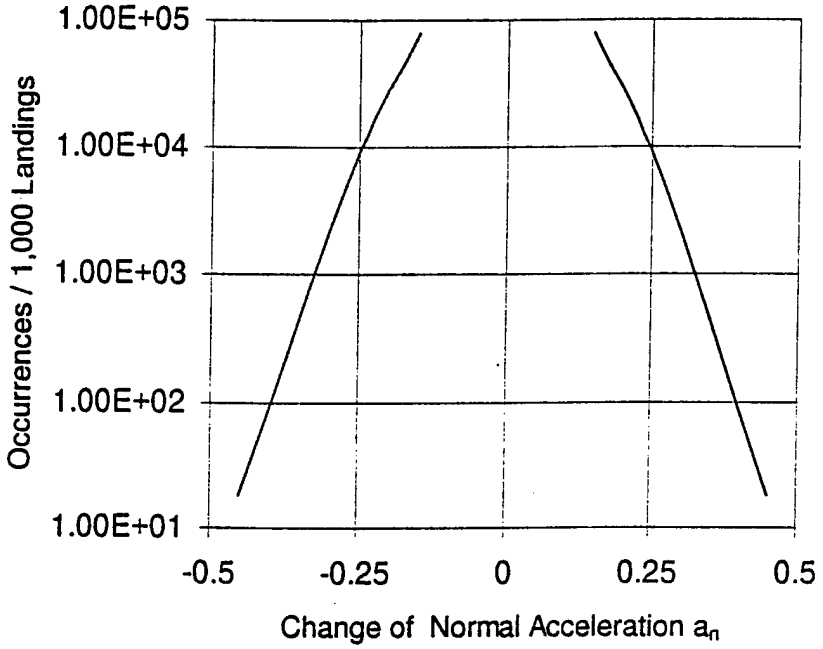

Figure B9. Exceedance Data of Taxi

B4.1.4 Differential Cabin Pressure

The pressure differential ΔP at an airplane altitude H_{plane} is the pressure difference between the cabin pressure P_{cabin} and the atmospheric pressure P_{atm}. The cabin pressure is generally expressed in terms of the cabin altitude H_{cabin}, which is limited to 8,000 feet under normal operating conditions as set forth in FAR 25.841. The atmospheric pressure at an altitude can be obtained from the Standard Atmosphere table published by ICAO International Civil Aviation Organization (Reference 3). It is assumed that the cabin altitude H_{cabin} is related to the airplane altitude H_{plane} in a parabolic form as described below:

$$H_{cabin} = C_p (H_{plane})^n$$

where H_{cabin} and H_{plane} are the cabin and airplane altitudes in feet, respectively, n is the cabin pressurization factor, and C_p is a coefficient calibrating the nominal maximum working pressure at the maximum airplane altitude. The cabin pressurization factor n takes a value of 1.6 in RAPIDC.

To determine the pressure differential Δp in psi at an airplane altitude in feet, the user provides RAPIDC with the maximum airplane altitude H_{max} in feet and the nominal maximum working pressure $p_{nominal,max}$ in psi. Using the steps as described below, RAPIDC calculates the pressure differential as a function of cruise atitude. In the calculation, the altitude and the pressure are in the units of feet and psi, respectively.

(1) Calculate the cabin altitude H_{cabin}

(a) Determine the maximum pressure $p_{H,max}$ at the maximum airplane altitude H_{max}
(b) Add the nominal maximum pressure $p_{nominal,max}$ to $p_{H,max}$ to obtain the cabin pressure p_{cabin}
(c) Determine the cabin altitude in feet H_{cabin} at cabin pressure p_{cabin}

(2) Calculate the coefficient C_p using the equation

$$C_p = \frac{H_{cabin}}{H_{max}^{1.6}}$$

(3) Calculate the pressure differential Δp

(a) Determine the atmospheric pressure P_{atm} at the airplane altitude H_{plane}
(b) Calculate the cabin altitude H_{cabin} and determine the cabin pressure p_{cabin}
(c) Calculate the pressure differential $\Delta p = p_{cabin} - p_{atm}$
(d) Add 0.6 psi to Δp per FAR 23.574

As an example, shown in Figure B10 below is the pressure schedule for an airplane providing a 9.3 psi nominal maximum working pressure at 45,000 feet airplane maximum altitude.

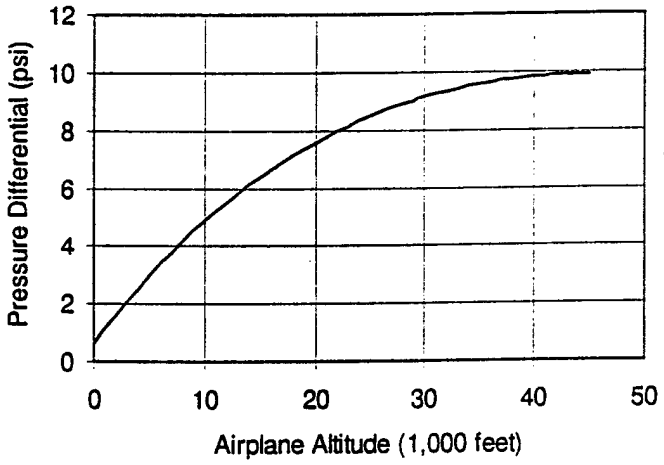

Figure B10. Example of Pressure Schedule

B4.2 Creation of Load Sequences

The load spectra are created according to the typical airplane operation profile described in Table B1 for commuters. The procedures of load spectrum generation

are coded in the FORTRAN computer program "CGENLINT" and are briefly described below:

1 Create load exceedance tables

The exceedance tables are calculated at 0.1g increments starting at 0.0g for a user specified number of flights for the gust and maneuver load environments. The exceedances are converted from nautical miles to exceedances per 1,000 flights based on the flight distance.

2 Create load occurrence tables

The occurrence tables are calculated at 0.1g increments starting at 0.15g based on the exceedances. The gust and maneuver occurrence tables per 1,000 flights are converted to occurrence tables per spectrum based on the user specified number of flights. Similarly, the taxi occurrence table per 1,000 landings is converted to occurrences per spectrum based on the user specified number of flights. For each load environment table, the total number of positive occurrences per spectrum and the total number of negative occurrences per spectrum should be equal. If any difference between the total numbers, it is correspondingly balanced at 0.0 Δg. The occurrence tables are also referred as "pool of load cycles".

3 Create load sequence for each flight profile stage

The load sequence is generated by randomly picking cycles from the appropriate pools for each flight profile stage. A Δg value is randomly picked from the positive pool of load cycles, and paired with another Δg value that is randomly picked from the negative pool of load cycles. Each cycle can only be picked once and every cycle in the pools is used. For each stage, the number of cycles to be picked is determined by the duration of that stage and the number of cycles in the pool as follows:

$$N_{pick} = \text{integer} \{ N_{pool} \times (T_{stage}/T_{pool}) \} + (1)_{nsf}$$

where

N_{pick} = number of cycles to be picked for the stage

N_{pool} = number of cycles in the original pool

T_{stage} = duration of the stage for one flight

T_{pool} = duration of the pool for a user specified number of flights

$+ (1)_{nsf}$ = additional cycle that is added to the flight every time the accumulation of the fraction portion of $\{N_{pool} \times (T_{stage}/T_{pool})\}$ becomes one cycle. The number of flights that have one additional cycle is determined as follows:

$nsf = N_{pool} - \text{integer}\{N_{pool} \times (T_{stage}/T_{pool})\} \times$ a user specified number of flights

In general, the cyclic loads are paired with respect to the 1-g state to form a full cycle. The order of load sequences for airborne stages are as follows: gust and maneuver. The minimum and maximum load factors and number of cycles for each operation environment are discussed in section B5.

B5. Contents of Load Spectrum

The generic load spectra are stored in binary form and can be retrieved using the following FORTRAN code:

```
      READ(iu) AN1,NSEG,(CPD(I),I=1,NSEG)
      READ(iu) NFLTS
      DO  I=1,NFLTS
          READ(iu) IFLT,IPAIR,((IDELTG(K,J),K=1,2),J=1,IPAIR),
     +         ((ICYC(K,J),K=1,NSEG),J=1,2)
      END DO
```

where

iu is the FORTRAN unit of the spectrum file

AN1 is the positive maneuver limit load factor

NSEG is the number of stages in the flight profile

CPD is the cabin pressure differentials for each stage of the flight profile; REAL*8

NFLTS is the total number of flights in the spectrum (i.e., default to 3,000)

IFLT is the flight number (i.e., 1 through 3,000)

IPAIR is the number of incremental load factors in the flight (max=2,000)

IDELTG is the array of incremental load factors; to save on storage, the incremental load factors are multiplied by 1000, truncated, and stored in the INTEGER*2 array

ICYC is the array of the summation count of the number of incremental load factors for each stage of the flight profile

B6. Derivation of Stress Spectrum

The stress spectrum at the location where the damage tolerance analysis is performed, in either the longitudinal or circumferential direction, can be derived from the load spectrum using the following equation:

$$\sigma = \sigma_p + (1 \pm \Delta g)\, \sigma_{lg}$$

Where σ is the min. or max. stress of a stress cycle in the stress spectrum

σ_p is the stress due to cabin pressure at the location

σ_{1g} is the 1-g stress due to airplane inertia and aerodynamic loads at the location

Δg is the change of normal acceleration in the unit of g's in the load spectrum

To estimate the longitudinal 1-g stress, σ_{1g} at the location where the damage tolerance analysis is performed, the following assumptions are made.

(1) The longitudinal stress in flight at the crown location can be described as shown in Figure B11. The stress in Zone I can be linearly interpolated within the zone.

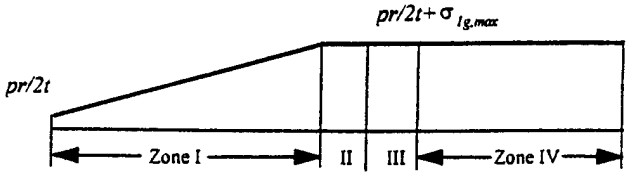

Figure B11 Longitudinal Stress in Flight at the Crown Location

(2) The longitudinal stress on the ground at the crown location can be described as shown in Figure B12. The stress in Zone II can be linearly interpolated within the zone.

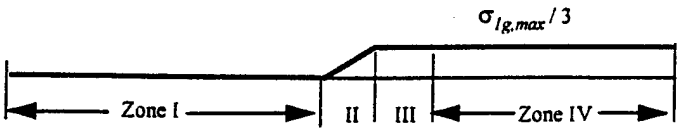

Figure B12. Longitudinal Stress on the Ground at the Crown Location

(3) The longitudinal stress between the crown and belly locations can be linearly interpolated as shown in Figure B13.

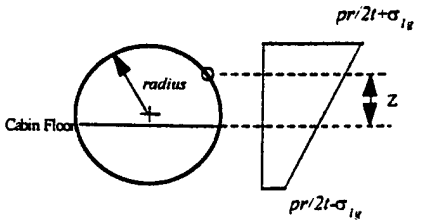

Figure B13. Longitudinal Stress at a Distance Z from cabin Floor

With these assumptions, the longitudinal stress at a location can be estimated once the maximum design 1-G stress, $\sigma_{1g,\,max}$ is determined. The determination of the $\sigma_{1g,\,max}$ is described as follows.

B6.1 Determination of Maximum Design 1-G Stress

It is assumed that the skin stress due to pressure and the maximum design 1-g stress, $\sigma_{1g,max}$ at the limit load is equal to the design limit stress of the fuselage skin. This assumption can be expressed in an equation as

$$\frac{(p+0.6)\,R}{2t} + n_1\,\sigma_{1g,\max} = C\,\frac{F_{tu}}{1.5}$$

where p is the pressure differential, n_1 is the maneuvering limit load factor, F_{tu} is the ultimate tensile strength of the skin material, C is the material allowable reduction factor for assembled structure, and R and t are fuselage radius and skin thickness at the location, respectively. The additional pressure 0.6 psi added to the pressure differential is to account for the external aerodynamic suction pressure (0.5 psi) plus regulator tolerance (0.1 psi) per FAR 23.574. In the above equation, n_1 is the positive maneuver limit load factor which can be calculated using the equation described in Section B4.1.1. An empirical value of 0.88 is used for the material allowable reduction factor, i.e., C=0.88.

Using the above equation, the maximum design 1-g stress, $\sigma_{1g,max}$ at the limit load can be determined as

$$\sigma_{1g,\max} = \frac{C \times \left(F_{tu} / 1.50 \right) - (p+0.6)\,R / 2t}{n_1}$$

For ground operation conditions, the maximum 1-g stress is assumed to be 1/3 of $\sigma_{1g,max}$ as shown in Figure B12.

B6.2 One-G Stress at Location of Interest

Once the maximum design 1-g stress, $\sigma_{1g,max}$ at the limit load is determined, the 1-g stress, σ_{1g} at a location of interest can be determined as follows.

(A) In-flight conditions

(i) Longitudinal stress in Zone I:

$$\sigma_{1g} = \lambda \left(\frac{Z}{R} \right) \left(\frac{L}{S} \right) \sigma_{1g,\max}$$

(ii) Longitudinal stress in Zones II, III, and IV:

$$\sigma_{1g} = \lambda \left(\frac{Z}{R}\right)\sigma_{1g,max}$$

(iii) Circumferential stress in all Zones:

$$\sigma_{1g} = 0$$

(B) Ground conditions

(i) Longitudinal stress in Zone I:

$$\sigma_{1g} = 0$$

(ii) Longitudinal stress in Zones II:

$$\sigma_{1g} = \lambda \frac{1}{3}\left(\frac{Z}{R}\right)\left(\frac{L}{S}\right)\sigma_{1g,max}$$

(iii) Longitudinal stress in Zones III and IV

$$\sigma_{1g} = \lambda \frac{1}{3}\left(\frac{Z}{R}\right)\sigma_{1g,max}$$

(iv) Circumferential stress in all Zones

$$\sigma_{1g} = 0$$

where

Z = the distance between the location and the cabin floor line, positive for locations above the floor line; negative for locations below the floor line

R = the radius of the fuselage

L = the distance between the location and the reference point in the zone (see Figure B1)

S = the length of zone (see Figure B1)

λ = assumed average payload factor equal to 0.70

B7. Rain-flow Count and Truncation

The stress sequences at the location is rain-flow counted for each flight and is truncated at the range of 2000 psi. The rain-flow counting method is one of the re-sequence processes generally applied to a flight-by-flight stress spectrum prior to the crack growth analysis. The method is illustrated in figure B13. Orienting the graphical display of the stress sequence vertically, the stress spectrum is regarded as a stack of tiles on the roof. Rain continues to flow from one tile to the next. If the water runs off the tile, it drops down on the tile below. It is assumed in this process that when the tile is already wet, the water stops to flow. Using this analogy, the stress range is regarded as the rain-flow range indicated by AB, CD, etc., in Figure B13. The rain-flow counting process has been standardized and is described in ASTM E-1049 (Reference 4).

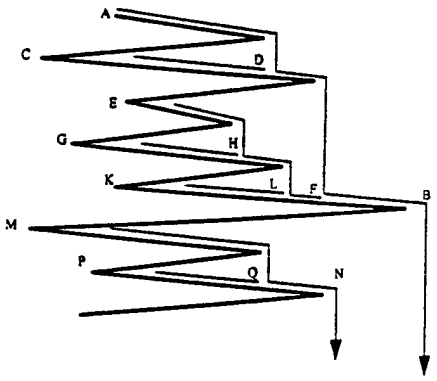

Figure B13. Rain-flow Count

The truncation of lower stress levels in a stress spectrum is employed in RAPIDC for efficiency in crack growth analysis. The stress truncation omits stress cycles below a certain magnitude. It is a general practice to accelerate the calculation. The argument is that low stress excursions do not contribute much to crack growth, especially in view of the retardation effects. The final stress sequences, after rain-flow counting and truncation, are used in the crack growth analysis.

References

1. General Aviation Aircraft-Normal Acceleration data Analysis and Collection Project, DOT/FAA/CT-91/20, FAA Technical Center, Atlantic City International Airport, NJ, February 1993

2. FAR Part 23, Appendix A

3. "Aerospace Design Engineer Guide," Pages 7-8, AIAA, January, 1987.

4. Standard Practice for Cycle Counting in Fatigue Analysis," ASTM E-1049-85.

Appendix C

One-Cycle Equivalent Stress Calculation

C1. Introduction

This appendix describes the derivation of the one-cycle equivalent stress for a stress spectrum either generated by RAPIDC or provided by the user. The one-cycle equivalent stress is used in the crack growth prediction of the modified skin to antenna installation using the simplified method.

C2. Derivation

In the crack growth analysis using the simplified method, the crack growth life N_{ij} for a crack growing from the size a_i to the size a_j ($a_j > a_i$) under a repeated flight can be calculated using the following equation [1]:

$$N_{ij} = \frac{1}{C}(SG_{ij})^{-p} \tag{1}$$

In equation 1, C and p are the coefficients in the Walker's crack growth equation,

$$\frac{da}{dN} = C\left\{(1-R)^q K_{Max}\right\}^p \tag{2}$$

where K_{max} is the stress-intensity factor evaluated at the stress σ_{Max} of the given stress cycle and R is the stress ratio of that cycle.

The parameter S in equation 1 is the one-cycle equivalent stress of the repeated flight, and G_{ij} is the geometry term pertinent to the crack geometry of the modified skin.

The equivalent stress S can be obtained by the equation:

$$S = \{\sum_{j=1}^{m}\left[\sigma_{Max,j}(1-R_j)^q\right]^p\}^{1/p} \tag{3}$$

where q is the coefficient in the Walker's crack growth equation, $\sigma_{Max,j}$ and R_j are the maximum stress and the stress ratio, respectively, of the j-th cycle, and m is the total number of cycles in the repeated flight.

The geometry term G_{ij} can be calculated by the equation:

$$G_{ij} = \{\int_{a_i}^{a_j}[\beta(a)\sqrt{\pi a}]^{-p}\,da\}^{-1/p} \tag{4}$$

where $\beta(a)$ is the geometry factor, and a is the crack length.

Suppose a stress spectrum at the antenna location contains M successive flights. Let m_j be the number of stress cycles in the j-th flight. A representative stress spectrum is depicted below in Figure 1.

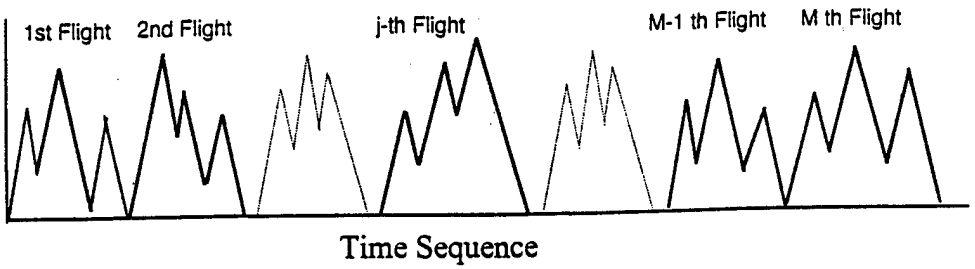

Figure 1. A Representative Stress Spectrum

With the stress spectrum in each flight prescribed, the one-cycle equivalent stress S_j for each j-th flight can be calculated using equation 3, and is schematically shown below in Figure 2.

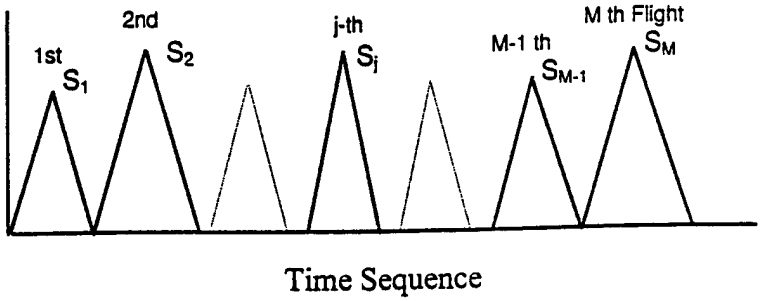

Figure 2. One-Cycle Equivalent Stress

Consider a stress spectrum containing M flights as shown in Figure 2. The equivalent stress S_{Eq} of a flight in the spectrum, as shown below in Figure 3

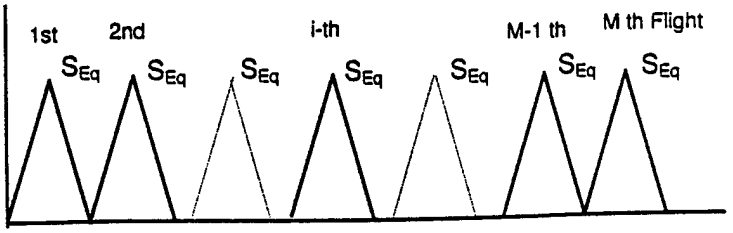

Figure 3. Equivalent Stress of M Flights

can be calculated as

$$S_{Eq} = \left(\frac{\sum_{i=1}^{M} S_i^p}{M} \right)^{1/p} \tag{5}$$

Substitution of equation 3 into equation 5 gives

$$S_{Eq} = \left(\frac{\sum_{i=1}^{M} \left\{ \sum_{j=1}^{m_i} \left[\sigma_{Max,j} (1 - R_j)^q \right]^p \right\}}{M} \right)^{1/p} \tag{6}$$

which can be rewritten as

$$S_{Eq} = \left(\frac{\sum_{k=1}^{n} \left[\sigma_{Max,k} (1 - R_k)^q \right]^p}{M} \right)^{1/p} \tag{7}$$

The variable n in equation 7 is the total number of stress cycles in the stress spectrum.

C3. Implementation and Validation

The calculation of the equivalent stress S_{Eq} for a stress spectrum containing M flights has been implemented in RAPIDC. The implementation was previously validated in RAPID, a precedent of RAPIDC, through an example. In order not to repeat the validation process, the previous example using a skin repair is reprinted as follows.

A skin repair with an external doubler mechanically fastened to the skin is shown below in Figure 4. The skin and repair doublers are made of the 2024-T3 clad sheet. Two fastener types, NAS1097-E6 and HL326-6 are used. Dimensions of the skin cutout and the repair doublers are given in the figure.

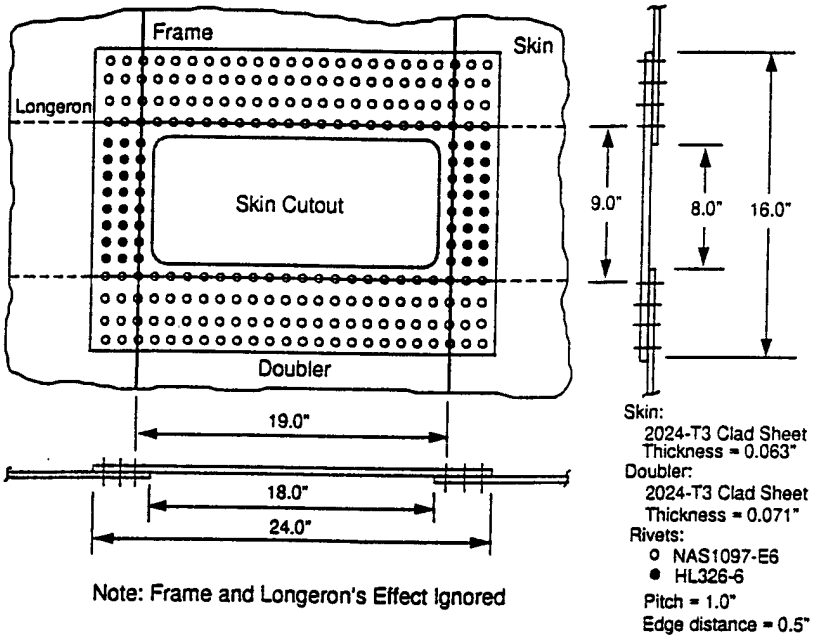

Figure 4. Description of the Example Repair

The radius near the repair is 120.0 inches, and the pressure differential is assumed to be 8.6 psi. To perform the crack growth analysis, an initial longitudinal skin crack of 0.05" is postulated at the critical center fastener hole in the first fastener row.

It is assumed that the skin near the repair location is subjected to a stress spectrum of 20,887 stress cycles representing 1/10 of the design life of the airplane. An overall spectrum summary is provided in the table 1 below.

Table 1 Overall Spectrum Summary

PEAK DISTRIBUTION		
Peak Stress		Cycles
Below -5000.		0
-5000.	-4000.	0
-4000.	-3000.	0
-3000	-2000.	0
-2000.	-1000.	0
-1000.	0.	0
0.	1000.	0
1000.	2000.	0
2000.	3000.	0
3000.	4000.	0
4000.	5000.	145
5000.	6000.	7358
6000.	7000.	1717
7000.	8000.	802
8000.	9000.	9697
9000.	10000.	1085
10000.	11000.	78
11000.	12000.	5
12000.	13000.	0
13000.	14000.	0
14000.	15000.	0
15000.	16000.	0
16000.	17000.	0
17000.	18000.	0
18000.	19000.	0
19000.	20000.	0
20000.	21000.	0
21000.	22000.	0
22000.	23000.	0
23000.	24000.	0
24000.	25000.	0
25000.	26000.	0
26000.	27000.	0
27000.	28000.	0
28000.	29000.	0
29000.	30000.	0
30000.	31000.	0
31000.	32000.	0
32000.	33000.	0
33000.	34000.	0
34000.	35000.	0
Above 35000.		0

RANGE DISTRIBUTION		
Stress Range		Cycles
Below 0.		
0.	1000.	0
1000.	2000.	0
2000.	3000.	14585
3000.	4000.	379
4000.	5000.	13
5000.	6000.	0
6000.	7000.	2361
7000.	8000.	3256
8000.	9000.	270
9000.	10000.	22
10000.	1000.	1
11000.	12000.	0
12000.	13000.	0
13000.	14000.	0
14000.	15000.	0
15000.	16000.	0
16000.	17000.	0
17000.	18000.	0
18000.	19000.	0
19000.	20000.	0
20000.	21000.	0
21000.	22000.	0
22000.	23000.	0
23000.	24000.	0
24000.	25000.	0
25000.	26000.	0
26000.	27000.	0
27000.	28000.	0
28000.	29000.	0
29000.	30000.	0
30000.	31000.	0
31000.	32000.	0
32000.	33000.	0
33000.	34000.	0
34000.	35000.	0
35000.	36000.	0
36000.	37000.	0
37000.	38000.	0
38000.	39000.	0
39000.	40000.	0
Above 40000.		0

STRESS RATIO DISTRIBUTION		
Stress Ratio		Cycles
Below -2.00		0
-2.00	-1.90	0
-1.90	-1.80	0
-1.80	-1.70	0
-1.70	-1.60	0
-1.60	-1.50	0
-1.50	-1.40	0
-1.40	-1.30	0
-1.30	-1.20	0
-1.20	-1.10	0
-1.10	-1.00	0
-1.00	-0.90	0
-0.90	-0.80	0
-0.80	-0.70	0
-0.70	-0.60	0
-0.60	-0.50	0
-0.50	-0.40	0
-0.40	-0.30	0
-0.30	-0.20	0
-0.20	-0.10	0
-0.10	0.00	0
0.00	0.10	0
0.10	0.20	4571
0.20	0.30	1340
0.30	0.40	17
0.40	0.50	126
0.50	0.60	2122
0.60	0.70	8453
0.70	0.80	4258
0.80	0.90	0
0.90	1.00	0
1.00	1.10	0
1.10	1.20	0
1.20	1.30	0
1.30	1.40	0
1.40	1.50	0
1.50	1.60	0
1.60	1.70	0
1.70	1.80	0
1.80	1.90	0
1.90	2.00	0
Above 0.0		0

Total Cycles	=	20887
Total No. of Flights	=	5910
Highest Peak	=	11760.30
Lowest Valley	=	1082.95
Largest Range	=	10283.55

To perform the crack growth analysis, it is assumed that a crack of size equal to 0.05" initially exists at the critical fastener hole in the skin. The crack grows towards the adjacent hole and enters the hole. When the crack grows into the hole, it is assumed that two equal-length cracks of 0.005" exist at outer holes. The crack continues to grow to enter next adjacent holes. The analysis proceeds until the residual strength of the repaired skin is no longer greater than the limit stress of the skin.

The scenarios for (a) a crack growing towards the adjacent hole and (b) continuing damage of the crack growing into the hole are depicted below in Figure 5.

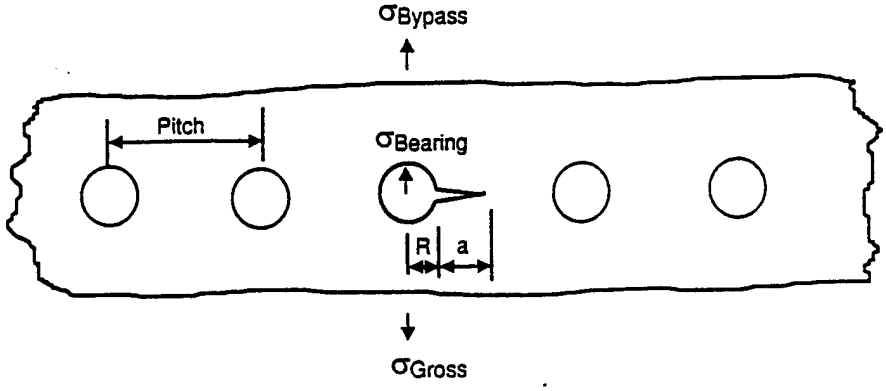

(a) Prior to Entering the Hole

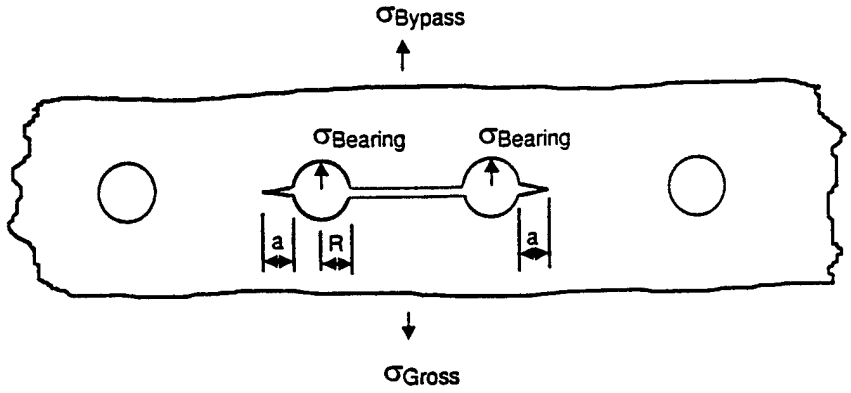

(b) Continuing Damage

Figure 5. Crack Growth Scenario

To perform the crack growth analysis using the simplified method, an equivalent stress S_{eq} equal to 11.915 ksi was calculated using equation 7. With this equivalent stress, RAPID calculates the crack growth. The analysis result was then compared with that obtained using the RAPID cycle-by-cycle method.

Crack growth analysis results obtained from RAPID using the equivalent stress in the simplified method and the cycle-by-cycle method, are plotted in Figure 6.

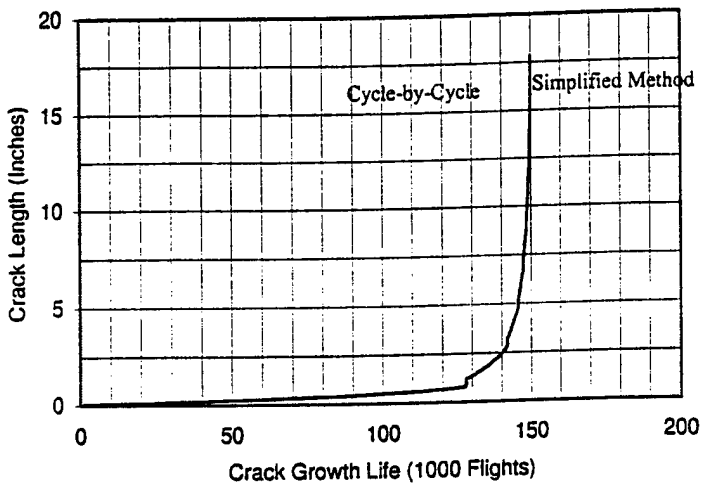

Figure 6. Crack Growth Life of the Example Repair

As shown in Figure 6, the crack growth obtained using the equivalent stress in the simplified method is nearly identical to that from the cycle-by-cycle method. In this analysis, the crack growth was calculated based on the zero stress ratio (R = 0.0) in the simplified method. The crack growth da/dN material data used in the cycle-by-cycle method were obtained for various stress R ratios using the Walker's equation. In this manner, the straight-line portion of the da/dN data were used in both analyses. Based on the analysis results shown in figure D6, it demonstrates that the simplified crack growth analysis method based on an equivalent stress converted from the stress spectrum produces the same crack growth life as that using the cycle-by-cycle method

Suppose the actual da/dN data, instead of that from the Walker's equation, were used in the cycle-by-cycle method. The crack growth life obtained is compared with that from the simplified method in Figure 7. It shows that the crack growth life obtained from the cycle-by-cycle method (144,757 flights) is about 3.5% shorter than that from the simplified method (149,850 flights).

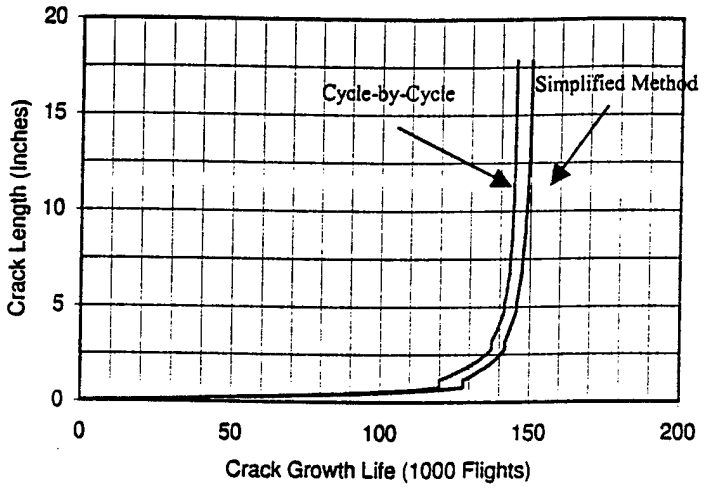

Figure 7. Crack Growth Life of the Example Repair

C4. Reference

1. T. Swift, "Repairs to Damage Tolerant Aircraft," Structural Integrity of Aging Airplanes, Edited by S. N. Atluri, S. G. Sampath, and P. Tong, Springer-Verlag, 1991, pp 433-483.